

1 **Effect of gas-transfer velocity parameterization choice on air-sea CO₂ fluxes in the North** 2 **Atlantic Ocean and the European Arctic**

3
4 Iwona Wrobel¹ and Jacek Piskozub¹

5
6 ¹ Institute of Oceanology, Polish Academy of Sciences, Sopot, Poland

7
8 *Correspondence to: I. Wróbel (iwrobel@iopan.gda.pl)*

9 10 11 Abstract

12
13 The oceanic sink of carbon dioxide (CO₂) is an important part of the global carbon budget.
14 Understanding uncertainties in the calculation of this net flux into the ocean is crucial for climate
15 research. One of the sources of the uncertainty within this calculation is the parameterization chosen
16 for the CO₂ gas transfer velocity. We used a recently developed software toolbox, called the
17 FluxEngine (Shutler et al., 2016), to estimate the monthly air-sea CO₂ fluxes for the extratropical
18 North Atlantic Ocean, including the European Arctic, and for the global ocean using several
19 published quadratic and cubic wind speed parameterizations of the gas transfer velocity. The aim of
20 the study is to constrain the uncertainty caused by the choice of parameterization in the North
21 Atlantic Ocean. This region is a large oceanic sink of CO₂, and it is also a region characterised by
22 strong winds, especially in winter but with good in situ data coverage. We show that the uncertainty
23 in the parameterization is smaller in the North Atlantic Ocean and the Arctic than in the global
24 ocean. It is as little as 5% in the North Atlantic and 4% in the European Arctic, in comparison to 9%
25 for the global ocean when restricted to parameterizations with quadratic wind dependence. This
26 uncertainty becomes 46%, 44% and 65%, respectively, when all parameterizations are considered.
27 We suggest that this smaller uncertainty (5% and 4%) is caused by a combination of higher than
28 global average wind speeds in the North Atlantic (> 7 ms⁻¹) and lack of any seasonal changes in the
29 direction of the flux direction within most of the region. We also compare the impact of using two
30 different *in situ* pCO₂ datasets (Takahashi et al. (2009) and SOCAT versions 1.5 and 2.0) for the
31 flux calculation. The annual fluxes using the two data sets differ by 8% in the North Atlantic and
32 19% in the European Arctic. The seasonal fluxes in the Arctic computed from the two datasets
33 disagree with each other possibly due to insufficient spatial and temporal data coverage, especially
34 in winter.

35 36 1. Introduction

37
38 The region of extratropical North Atlantic Ocean, including the European Arctic, is a region
39 responsible for the formation of deep ocean waters (see Talley (2013) for a recent review). This
40 process, part of the global overturning circulation, makes the area a large sink of atmospheric CO₂
41 (Takahashi et al., 2002; Takahashi et al., 2009; Landschützer et al., 2014; Le Quéré et al., 2015).
42 Therefore, there is a widespread interest in tracking the changes in the North Atlantic net carbon
43 dioxide fluxes, especially as models appear to predict a decrease in the sink volume later this
44 century (Halloran et al., 2015).

45
46 The trend and variations in the North Atlantic CO₂ sinks has been intensively studied since
47 observations have shown it appeared to be decreasing (Lefèvre et al., 2004). This decrease on inter-
48 annual time scales has been confirmed by further studies (Schuster and Watson, 2007) and this trend
49 has continued in recent years North of 40° N (Landschützer et al., 2013). It is not certain how many
50 of these changes are the result of long-term changes, decadal changes in atmospheric forcing-
51 namely the North Atlantic Oscillation (González-Dávila et al., 2007; Thomas et al., 2008; Gruber
52 2009; Watson et al., 2009) or changes in meridional overturning circulations (Pérez et al., 2013).

53 Recent assessments of the Atlantic and the Arctic net sea-air CO₂ fluxes (Schuster et al., 2013) and
54 the global ocean net carbon uptake (Wanninkhof et al., 2013) show that the cause is still unknown.

55
56 To study the rate of the ocean CO₂ sink and especially its long-term trend, one needs to first
57 constrain the uncertainty in the flux calculation. The global interannual variability in air-sea CO₂
58 fluxes can be about 60% due to differences in $p\text{CO}_2$ and 35% by gas transfer velocity k
59 parameterization (Couldrey et al., 2016). Sources of uncertainty include sampling coverage, the
60 method of data interpolation, data quality of the fugacity of CO₂ ($f\text{CO}_2$), the method used for
61 normalization of fugacity data to a reference year in a world of ever increasing atmospheric CO₂ the
62 measurement uncertainty in all the parameters used to calculate the fluxes (including partial
63 pressure in water and air, bulk and skin water temperatures, air temperatures, wind speed etc.) and
64 some which are not usually included in the calculations but most probably influence the flux values
65 (sea state parameters, air bubble void fraction, surfactant effects etc.) as well as the choice of gas
66 transfer velocity k parameterization formula (Landschützer et al., 2014; Woolf et al., 2015a, 2015b).
67 It has also been identified that the choice of the wind data product provides an additional source of
68 uncertainty in gas transfer velocity, even by 10% - 40%, and the choice of the wind speed
69 parameterization may cause variability in k as much as about 50% (Gregg et al., 2014; Couldrey et
70 al., 2016). In this work we have analyzed solely the effects of the choice between various published
71 empirical winds driven gas transfer parameterizations. The North Atlantic is one of the regions of
72 the world ocean best covered by CO₂ fugacity measurements (Watson et al., 2011), the Arctic seas
73 coverage is much poorer, especially in winter (Schuster et al., 2013).

74
75 In the literature there are many different parameterizations to choose from and most depend on a
76 cubic or quadratic wind speed relationship. The choice of the appropriate parameterization is not
77 trivial as indicated by the name of an international meeting which focused on this topic (“ k
78 conundrum” workshop, COST-735 Action organized meeting in Norwich, February 2008). The
79 conclusions from this meeting have been incorporated into a recent review book chapter (Garbe et
80 al., 2014). This paper concentrates on quantifying the uncertainty caused by the choice of the gas
81 transfer velocity parameterization in the North Atlantic and the European Arctic. These regions
82 were chosen as they are the areas for which many of the parameterizations were originally derived.
83 They are also regions with wind fields skewed towards higher winds (in comparison to the global
84 average) enabling the effect of stronger winds on the net flux calculations to be investigated by
85 using published gas transfer velocity formulas.

86 87 2. Methods

88 89 2.1 Datasets

90
91 We calculated net air-sea CO₂ fluxes using a set of software processing tools called the
92 ‘FluxEngine’ (Shutler et al., 2016), which was created as part of European Space Agency funded
93 OceanFlux Greenhouse Gases project (<http://www.oceanflux-ghg.org>). The tools were developed to
94 provide the community with a verified and consistent toolbox and to encourage the use of satellite
95 Earth Observation (EO) data for studying air-sea fluxes. The toolbox source code can be
96 downloaded or alternatively there is a version that can be run through a web interface. Within the
97 online web interface, a suite of reanalysis data products, *in situ* and model data are available as
98 input to the toolbox. The FluxEngine allows the users to select several different air-sea flux
99 parameterizations producing monthly global gridded net air-sea fluxes products with 1° x 1° spatial
100 resolution. The output consists of twelve NetCDF files (one file per month). One monthly
101 composite file includes the mean (first order moment), median, standard deviation and the second,
102 third and fourth order moments. There is also information (meta data) about origin of data inputs.
103 For example, the monthly EO input data include: rain intensity, wind speed and direction, % of sea
104 ice cover from monthly model data, ECMWF air pressure, whitecapping (Goddijn-Murphy et al.,

105 2011), two options for monthly datasets of $p\text{CO}_2$, Sea Surface Temperature (SST), salinity. The user
106 then needs to choose the different components and structure of the net air-sea gas flux calculation
107 and choose the transfer velocity parameterization.

108 For the calculations, we used $p\text{CO}_2$ and salinity values from Takahashi et al. (2009) climatology
109 which was based on more than 3 million measurements of surface water $p\text{CO}_2$ in open-ocean
110 environments during non El Nino conditions. For some calculations we used, as an alternative,
111 Surface Ocean CO_2 Atlas (SOCAT) version 1.5 and 2.0 (Sabine et al., 2013; Pfeil et al., 2013;
112 Bakker et al., 2014) $p\text{CO}_2$ and associated SST data. SOCAT is a community driven dataset
113 containing 6.3 and 10.1 million surface water CO_2 fugacity values for version 1.5 and 2.0,
114 respectively, with a global coverage. The SOCAT databases have been re-analysed and then
115 converted to climatologies using the methodology described in Goddijn-Murphy et al. (2015). All
116 the climatologies were calculated for year 2010 with the FluxEngine toolset. The SSTskin (defined
117 within Group for High Resolution SST (GHRSSST) as temperature of the surface measured by an
118 infrared radiometer operating at the depth of $\sim 10\text{-}20\ \mu\text{m}$) values were taken from the Advance
119 Along Track Scanning Radiometer (ESA/ARC/(A)ATSR) Global Monthly Sea Surface dataset
120 (Merchant et al., 2012) in the case of both datasets, and have been preprocessed in the same way for
121 use with the FluxEngine (Shutler et al., 2016).

122
123 We used Earth Observation (EO) wind speed and sea roughness (σ_0 – altimeter backscatter signal in
124 Ku band from GlobWave L2P products) data obtained from the European Space Agency (ESA).
125 The GlobWave satellite products give a “uniform” set of along track satellite wave data from all
126 available Altimeters (spanning multiple space agencies) and from ESA Synthetic Aperture Radar
127 (SAR) data and are publicly available at the Ifremer/CERSAT cloud
128 (<http://globwave.ifremer.fr/products/data-access>). Wave data are collected from six altimeter
129 missions (Topex/POSEIDON, Jason-1/22, CryoSAT, GEOSAT and GEOSAT Follow On) and
130 from ESA Synthetic Aperture Radar (SAR) missions, namely ERS-1/2 and ENVISAT. All data
131 come in netCDF-3 format.

132
133 All analyses were performed using global data contained in the FluxEngine software. From the
134 gridded product ($1^\circ \times 1^\circ$) we extracted data from the extratropical North Atlantic Ocean (north of
135 30°N), and its subset, the European Arctic (north of 64°N). For comparison, we also calculated
136 fluxes in the Southern Ocean (south of 40°S). Hereafter we follow the convention of that sources of
137 CO_2 (upward ocean-to-atmosphere gas fluxes) are positive and sinks (downward atmosphere-to-
138 ocean gas fluxes) are negative. We give all results of net CO_2 fluxes in the SI unit of Pg (Pg is 10^{15}
139 g which is numerically identical to Gt).

140 141 2.2. k parameterizations

142
143 The flux of CO_2 at the interface of air and the sea is controlled by wind speed, sea state, sea
144 surface temperature (SST) and other factors. We estimate the net air-sea flux of CO_2 (F , mg C m^{-2}
145 day^{-1}) as the product of gas transfer velocity (k , ms^{-1}) and the difference in CO_2 concentration
146 (gm^{-3}) in the sea water and its interface with the air (Land et al., 2013). The concentration of CO_2 in
147 sea water is the product of its solubility (α , $\text{gm}^{-3}\ \mu\text{atm}^{-1}$) and its fugacity ($f\text{CO}_2$, μatm). Solubility is
148 in turn, a function of salinity and temperature. Hence F is defined as:

$$149
150 F = k (\alpha_W f\text{CO}_{2W} - \alpha_S f\text{CO}_{2A}) \quad (1)$$

151
152 where the subscripts denote values in water (W) and the air-sea interface (S) and in the air (A). We
153 can exchange fugacity with the partial pressure (their values differ by $<0.5\%$ over the temperature
154 range considered) (McGillis et al., 2001). So equation (1) now becomes:

$$155
156 F = k (\alpha_W p\text{CO}_{2W} - \alpha_S p\text{CO}_{2A}) \quad (2)$$

157

158 One can also ignore the differences between the two solubilities, and just use the waterside solubility
159 α_w . Equation (2) will then become:

160

$$161 \quad F = k \alpha_w (p\text{CO}_{2W} - p\text{CO}_{2A}) \quad (3)$$

162

163 This formulation is often referred to as the ‘bulk parametrization’.

164

165 In this study we chose to analyze the air-sea gas fluxes using five different gas transfer
166 parameterizations (k). All of them are wind speed parameterizations, but differ in the formula used:

167

$$168 \quad k = \sqrt{(660.0 / \text{Sc}_{\text{skin}})} * (0.212 U_{10}^2 + 0.318 U_{10}) \quad (4)$$

(Nightingale et al., 2000),

169

$$171 \quad k = \sqrt{(660.0 / \text{Sc}_{\text{skin}})} * 0.254 U_{10}^2 \quad (5)$$

(Ho et al., 2006),

172

$$174 \quad k = \sqrt{(660.0 / \text{Sc}_{\text{skin}})} * 0.0283 U_{10}^3 \quad (6)$$

(Wanninkhof and McGillis, 1999),

175

$$177 \quad k = \sqrt{(660.0 / \text{Sc}_{\text{skin}})} * 0.251 U_{10}^2 \quad (7)$$

(Wanninkhof, 2014),

178

$$180 \quad k = \sqrt{(660.0 / \text{Sc}_{\text{skin}})} * (3.3 + 0.026 U_{10}^3) \quad (8)$$

(McGillis et al., 2001),

181

182

183 where Sc_{skin} stands for the Schmidt numbers at the skin surface, a function of SST ($[= (\text{kinematic}$
184 $\text{viscosity of water})/(\text{diffusion coefficient of CO}_2 \text{ in water})]$), 660.0 is the Schmidt number
185 corresponding to values of carbon dioxide at 20 °C in seawater, U_{10} is the wind speed 10 m above
186 the sea surface.

187

188 In addition to the purely wind driven parameterizations, we have used the combined Goddijn-
189 Murphy et al. (2012) and Fangohr and Woolf (2007) parameterization, which was developed as a
190 test algorithm within of OceanFlux GHG Evolution project. This parameterization separates
191 contributions from direct- and bubble-mediated gas transfer as suggested by Woolf (2005). Its
192 purpose is to enable a separate evaluation of the effect of the two processes on air-sea gas fluxes
193 and it is an algorithm that has yet to be calibrated. We used two versions of this parameterization:
194 wind driven direct transfer (using the U_{10} wind fields) and radar backscatter driven direct transfer
195 (using mean wave square slope) as described in Goddijn-Murphy et al. (2012).

196

197 3. Results

198

199 Using the FluxEngine software, we have produced global gridded monthly net CO₂ air-sea fluxes
200 and from these we have extracted the values for the two study regions, the extratropical North
201 Atlantic Ocean and separately for its subset - the European Arctic seas. Figure 1 shows maps of the
202 monthly mean air-sea CO₂ fluxes for the North Atlantic, calculated with Nightingale et al. (2000)
203 (hereafter called N2000) k parameterization and the Takahashi et al. (2009) climatology for the
204 whole year and for each season. The area, as a whole, is a sink of CO₂ but some regions close to
205 North Atlantic Drift and East Greenland Current (Figure 2) are net sources. At the seasonal maps
206 one can see more variability affects by physical process (with temperature changes causing
207 maximum in-water pCO₂ in summer) or biological activity (with phytoplankton blooms causing

208 summer values to be lowest in the annual cycle). For example, the areas close to the North Atlantic
209 Drift And East Greenland current are sinks of CO₂ in the summer (likely due to the growth of
210 phytoplankton) while the southern most areas of the region become CO₂ sources in summer and
211 autumn (which is likely to be due to the effect of sea-water temperature changes). Much of this
212 variability is caused by changes of the surface water $p\text{CO}_2$ values, shown in Figure 3 for the whole
213 year and for each season (and variability in atmospheric CO₂ partial pressure, not shown). However,
214 the flux is proportional to the product of $\Delta p\text{CO}_2$ and k . In most parameterizations k is a function of
215 wind speed (eqs. 4-8). The mean wind speed U_{10} for the whole year and each season are shown in
216 Figure 4. The wind speeds in the North Atlantic are higher than the mean value in the world ocean
217 (which is 7 m s^{-1} ; Couldrey et al., 2016), with mean values higher than 10 m s^{-1} in many regions of
218 the study area in all seasons except for the summer (with highest values in winter). This is important
219 because the air-sea flux depends not only on average wind speed but also on its distribution (see
220 Discussion below). This effect is especially visible between formulas with different powers of U_{10} .
221 Figure 5 shows the difference in the air-sea CO₂ fluxes calculated using two example
222 parameterizations: one proportional to U_{10}^3 (eq. 6) and one to U_{10}^2 (eq. 7), namely Wanninkhof and
223 McGillis (1999) (hereafter called WMcG1999) and Wanninkhof (2014) (hereafter called W2014). It
224 can be seen that the “cubic” function results in higher absolute air-sea flux values when compared
225 to the “quadratic” function in the regions of high winds, and lower absolute air-sea flux values in
226 weaker winds.

227
228 Figure 6 shows the monthly values of air-sea CO₂ fluxes for the five parameterizations (eq. 4-8) for
229 the North Atlantic and the European Arctic. The regions are sinks of CO₂ in every month, although
230 August is close to neutral for the North Atlantic. The results using cubic parameterizations (eqs. 6
231 and 8) are higher in absolute values, by up to 30% for WMcG1999 and 55% for McGillis (2001)
232 (hereafter called McG2001), in comparison to the “quadratic” of N2000 (eq. 4). The other two
233 “quadratic” parameterizations W2014 and Ho et al. (2006) (hereafter called H2006) (eqs. 5 and 7)
234 resulted in fluxes within 5% of N2000. In addition to the five parameterizations Figure 7 presents
235 results for both of the OceanFlux GHG Evolution formulas (using wind and radar backscatter data).
236 The mean and standard deviations of the parameterization ensemble are shown as grey vertical
237 lines. The standard deviation in global fluxes is similar to previous estimates (Sweeney et al., 2007,
238 Landschützer et al., 2014) but they cannot be directly compared due to different parameterization
239 choices and methodologies. Annual net fluxes for the North Atlantic, Southern and global ocean as
240 well as for the European Arctic are shown in Table 1. The results show that the annual North
241 Atlantic net air-sea CO₂ sink, depending on the formula used, varies from -0.38 Pg C for N2000 to -
242 0.56 Pg C for McG2001. In the case of global net air-sea CO₂ sink the values are -1.30 Pg C and -
243 2.15 Pg C, respectively. Table 1 as well as Figure 7 shows the same data “normalized” to the N2000
244 data (divided by value), which allows us to visualize the relative differences (in Table 1 values in
245 parentheses). In the case of the North Atlantic using the “quadratic” W2014 and H2006
246 parameterizations results in a net air-sea flux that are 4% and 5% higher in absolute values,
247 respectively, than the equivalent N2000 result, while the “cubic” WMcG1999 and McG2000 results
248 in values that are 28% and 44% higher, respectively, than N2000 results, for this regions. The
249 respective values for the Arctic are 3% for W2014 and 4% for H2006, as well as 28% for
250 WMcG1999 and 44% for McG2001 than N2000. In the case of global net air-sea CO₂ fluxes the
251 equivalent values are 8% (W2014) and 9% (H2006) higher than the N2000 result for the quadratic
252 functions as well as 33% (WMcG1999) and 65% (McG2001) for cubic ones. The OceanFlux GHG
253 parameterization for the backscatter and wind-driven versions, results in net air-sea CO₂ fluxes
254 higher for North Atlantic Ocean than the N2000, that are 38% and 47%, respectively, and in the
255 global case the values, for those two versions, were 44% and 52% higher, respectively, than N2000
256 values. The spread of the Arctic values was lower than that of the Atlantic ones (see Table 1). On
257 the other hand, the values for the Southern Ocean were slightly higher than for the North Atlantic
258 but lower than the global ones, with the exception of the OceanFlux GHG parameterizations.

259

260 All the above results were obtained with the Takahashi et al. (2009) $p\text{CO}_2$ climatology and for
 261 comparison, we have also calculated the air-sea CO_2 fluxes using the re-analysed SOCAT versions
 262 1.5 and 2.0 data (which were converted to climatologies using methodology described in Goddijn-
 263 Murphy et al., 2015). Figure 8 shows the results using the N2000 k parameterization for all three of
 264 the datasets (Takahashi et al. (2009) and both SOCAT versions). In the case of the North Atlantic
 265 Ocean study area, although the monthly values show large differences (using both SOCAT datasets
 266 results in a larger sink in summer and smaller in winter compare to Takahashi et al. (2009)), the
 267 annual values are similar: -0.38 Pg C for both Takahashi et al. (2009) and SOCAT v1.5 and -0.41 Pg
 268 C for SOCAT v2.0. In the case of the European Arctic the situation is very different, with Takahashi
 269 et al. (2009) and SOCAT dataset derived climatologies resulting in inverse seasonal variability but
 270 with annual net air-sea CO_2 fluxes results that are similar: -0.102 Pg C for Takahashi et al. (2009), $-$
 271 0.085 Pg C for SOCAT v1.5 and -0.088 Pg C for SOCAT v2.0.

272 273 4. Discussion

274
275 Our results show that using the three “quadratic” parameterizations (Nightingale et al., 2000; Ho et
 276 al., 2006 and Wanninkhof, 2014) air-sea fluxes are within 5% of each other in the case of the North
 277 Atlantic (Table 1, values in parentheses). This discrepancy is smaller than the 9% difference
 278 identified for the global case (Table 1 and Fig. 7). This confirms that at present, these different
 279 parameterizations are interchangeable for the North Atlantic as this range is within the experimental
 280 uncertainty (Nightingale, 2015). The three parameterizations were derived using different methods
 281 and data from different regions, namely passive tracers and dual-trace experiments in the North Sea
 282 in the case of Nightingale et al. (2000), dual tracers in the Southern Ocean in the case of Ho et al.
 283 (2006), and global ocean ^{14}C inventories in the case of Wanninkhof (2014). The differences between
 284 the quadratic and cubic parameterization are large, and instead of the quadratic functions that are
 285 supported by several lines of evidence (see Garbe et. al., 2014 for discussion), the cubic function are
 286 not completely refuted by the available observation. Therefore, it is important to notice that a choice
 287 of one of the available cubic functions may leads to net air-sea CO_2 fluxes that are considerably
 288 larger in absolute values, by up to 33% in the North Atlantic Ocean and more than 50% in the
 289 global ocean.

290
291 The above results imply smaller relative differences between the parameterizations in the North
 292 Atlantic Ocean than in the global ocean. This is interesting because the North Atlantic is the region
 293 of strong winds and over most of its area there are no seasonal changes in the air-sea flux direction
 294 (Fig. 1). For example in the South Atlantic, the annual mean wind speed is 8.5 m s^{-1} which is lower
 295 values of wind speed than in the North Atlantic (9 m s^{-1}) and the range of seasonal changes in the
 296 air-sea CO_2 fluxes are from -0.05 to $+0.05 \text{ Pg C yr}^{-1}$ with difference between parameterizations
 297 lower than in the North Atlantic (Le Quèrè et al., 2007; Takahashi et al., 2009). Takahashi et al.
 298 (2009) also indicate that the air-sea CO_2 fluxes difference in the Southern Ocean is strongly
 299 dependent on the choice of the gas transfer parameterizations and wind speed. Smaller differences
 300 in the North Atlantic Ocean than in the global ocean are surprising, given that at least some of the
 301 older parameterizations (e.g. W2009 or WMcG1999) were developed using a smaller range of
 302 winds than what occurs in the North Atlantic. There may be two reasons for this. First, when
 303 comparing quadratic and cubic parameterizations (Fig. 9), the cubic parameterization implies higher
 304 air-sea fluxes for high winds, whereas the quadratic ones lead to higher fluxes for weaker winds.
 305 This difference can be presented in arithmetic terms. Let us assume two functions of wind speed U ,
 306 $F_1(U)$ quadratic and $F_2(U)$ cubic:

$$307 \quad F_1(U) = a U^2, \quad (9)$$

$$308 \quad F_2(U) = b U^3. \quad (10)$$

309
310
311

312 The difference between the two functions ΔF is equal to:

$$\Delta F = F_2 - F_1 = b U^3 - a U^2 = b U^2 (U - a b^{-1}) = b U^2 (U - U_x) \quad (11)$$

315 where $U_x = a b^{-1}$. The difference is positive for wind speeds greater than U_x and negative for winds
316 less than U_x . U_x is the value of wind speed for which the two functions intersect. In the case of
317 equations (6) and (7), where $a = 0.251$ and $b = 0.0283$, they imply that $U_x = 8.87 \text{ m s}^{-1}$. In fact all of
318 the functions presented in Fig. 9 produce very similar values for U_x , all of which are close to 9 m s^{-1} .
319 This value is very close to average wind speed in the North Atlantic (Fig. 4). This is one of the
320 reasons of the small relative difference in net air-sea fluxes. The spread of flux values for the
321 Southern Ocean seems to support this conclusion, being larger than that in the North Atlantic. The
322 Southern Ocean has on average stronger winds than the North Atlantic (including also the Arctic
323 Seas) which seems to have the smallest spread of flux values for different parameterizations. The
324 other reason of smaller relative differences between the parameterizations in the North Atlantic than
325 in the global ocean is the lack of seasonal variation in the sign of the air-sea flux. In the case of
326 seasonal changes in the air-sea flux direction (caused by seasonal changes in water temperature or
327 primary productivity), with winds stronger than U_x in some seasons and weaker in others (usually
328 strong winds in winter and weak in summer), the fluxes partly cancel each other. The difference
329 between cubic and quadratic parameterizations adds to each other due to simultaneous changes in
330 the sign of both fluxes itself and the $U - U_x$ term. This effect of seasonal variation has been
331 suggested to us based on available observations (A. Watson, University of Exeter– personal
332 communication) but we are unaware of any paper investigating it or even describing it explicitly.
333
334

335 In addition to the five parameterizations described above, we calculated the air-sea fluxes using the
336 OceanFlux GHG Evolution combined formula, which is based on knowledge that air-sea exchange
337 is enhanced by air-entraining wave breaking and bubble-mediated transfer, especially for the less
338 soluble gases than CO_2 . Goddijn-Murphy et al. (2016) assume a linear wind relationship for
339 dimethyl sulphide (DMS) and an additional bubble-mediated term for less soluble gases,
340 parameterized with whitecap coverage. The resulting air-sea fluxes are higher in absolute terms,
341 than all of the quadratic functions considered in this study, and are closer in value to cubic
342 parameterization. This may mean that the bubble mediated term of Fangohr and Woolf (2007) is
343 overestimating the bubble component, implying the need for a dedicated calibration effort. This
344 question will be the subject of further studies in the OceanFlux GHG Evolution project.
345

346 Using both Takahashi et al. (2009) climatology and SOCAT datasets (Fig. 8) results in similar
347 annual net air-sea CO_2 fluxes in the North Atlantic; however it should be noted that they show
348 different seasonal variations. This may have been caused by slightly different time periods of the
349 datasets as the SOCAT-based dataset contains more recent data. It should be noted that a significant
350 part of the data from Takahashi et al. (2009) are included in SOCAT so the differences in the
351 European Arctic may be due to the sparse data coverage and possible interpolation artifacts
352 (Goddijn-Murphy et al., 2015) or to processing of the data through the FluxEngine. A recent paper
353 (Couldrey et al., 2016) using even more high latitude data than were available in the SOCAT
354 versions 1.5 and 2.0, which we used, shows similar seasonal pattern as SOCAT. Still, this
355 discrepancy makes us treat the net air-sea CO_2 fluxes results from the Arctic with much less
356 confidence than the values for the whole North Atlantic. It is impossible to decide in this study
357 which dataset is more accurate as only new data can settle this. However, new data, not included in
358 the SOCAT versions we used, have been available to the recent analysis by Yasunaka et al. (2016).
359 The observed $p\text{CO}_2$ data (Fig. 4 in Yasunaka et al., 2016), especially since 2005, show clearly an
360 annual cycle compatible with the SOCAT seasonal flux variability.
361

362 5. Conclusions

363

364 In this paper we have studied the effect of the choice of gas transfer velocity parameterization on
365 the net CO₂ air-sea gas fluxes in the North Atlantic and the European Arctic using the recently
366 developed FluxEngine software. The results show that the uncertainty caused by the choice of the *k*
367 formula is smaller in the North Atlantic and in the Arctic than it is globally. The difference in the
368 annual net air-sea CO₂ fluxes caused by the choice of the parameterization is 5% in the North
369 Atlantic and 4% in the European Arctic, comparing to 9% globally for the studied functions with
370 quadratic wind dependence. It is up to 46% different for the North Atlantic, 36% for the Arctic and
371 65% globally when comparing cubic and quadratic functions. In both cases the uncertainty in the
372 North Atlantic and the Arctic regions are smaller than the global case. We explain the smaller North
373 Atlantic variability to be a combination of, firstly, higher than global average wind speeds in the
374 North Atlantic, close to 9 m s⁻¹, which is the wind speed at which most *k* parameterization have
375 similar values, and secondly the all-season CO₂ sink conditions in most North Atlantic areas. We
376 repeated the analysis using Takahashi et al. (2009) and SOCAT *p*CO₂ derived climatology and find
377 that although the seasonal variability in the North Atlantic is different the annual net air-sea CO₂
378 fluxes are within 8% in the North Atlantic and 19% in the European Arctic. The seasonal flux
379 calculated from the two *p*CO₂ datasets in the Arctic have inverse seasonal variations, indicating
380 possible under sampling (aliasing) of the *p*CO₂ in this polar region and therefore highlighting the
381 need to collect more polar *p*CO₂ observations in all months and seasons.
382
383
384

385 Acknowledgements

386
387 The publication has been financed from the funds of the Leading National Research Centre
388 (KNOW) received by the Centre for Polar Studies for the period 2014-2018; OceanFlux
389 Greenhouse Gases Evolution, a project funded by the European Space Agency, ESRIN Contract No.
390 4000112091/14/I-LG; and GAME "Growing of Marine Arctic Ecosystem", funded by Narodowe
391 Centrum Nauki grant DEC-2012/04/A/NZ8/00661. We would also like to thank Jamie Shutler for
392 important advice on the FluxEngine and for correcting the manuscript for English language. The
393 authors are very grateful to those who have produced and made freely available the LDEO Flux
394 Climatology base, FluxEngine software funded by European Space Agency, Surface Ocean CO₂
395 Atlas (SOCAT), GlobWave Project funded by European Space Agency, as well as Centre de
396 Recherché et d'Exploitation Satellitaire (CERSAT) at IFREMER.
397
398

399 References

400
401 Bakker, D. C. E., Pfeil, B., Smith, K., Hankin, S., Olsen, A., Alin, S. R., Cosca, C., Harasawa, S.,
402 Kozyr, A., Nojiri, Y., O'Brien, K. M., Schuster, U., Telszewski, M., Tilbrook, B., Wada, C., Akl,
403 J., Barbero, L., Bates, N. R., Boutin, J., Bozec, Y., Cai, W.-J., Castle, R. D., Chavez, F. P., Chen,
404 L., Chierici, M., Currie, K., De Baar, H. J. W., Evans, W., Feely, R. A., Fransson, A., Gao, Z.,
405 Hales, B., Hardman-Mountford, N. J., Hoppema, M., Huang, W.-J., Hunt, C. W., Huss, B.,
406 Ichikawa, T., Johannessen, T., Jones, E. M., Jones, S. D., Jutterstrom, S., Kitidis, V., Kortzinger,
407 A., Landschützer, P., Lauvset, S. K., Lefèvre, N., Manke, A. B., Mathis, J. T., Merlivat, L., Metzl,
408 N., Murata, A., Newberger, T., Omar, A. M., Ono, T., Park, G.-H., Paterson, K., Pierrot, D., Ríos,
409 A. F., Sabine, C. L., Saito, S., Salisbury, J., Sarma, V. V. S. S., Schlitzer, R., Sieger, R., Skjelvan,
410 I., Steinhoff, T., Sullivan, K. F., Sun, H., Sutton, A. J., Suzuki, T., Sweeney, C., Takahashi, T.,
411 Tjiputra, J., Tsurushima, N., van Heuven, S. M. A. C., Vandemark, D., Vlahos, P., Wallace, D. W.
412 R., Wanninkhof, R., and Watson, A. J.: An update to the Surface Ocean CO₂ Atlas (SOCAT
413 version 2), *Earth Syst. Sci. Data*, 6: 69-90, doi:10.5194/essd-6-69-2014, 2014.
414

415 Couldrey, M. P., Oliver, K. I. C., Yool, A., Halloran, P. R., Achterberg, E. P.: On which timescale do

416 gas transfer velocities control North Atlantic CO₂ flux variability?, *Global Biogeochem. Cycles*,
417

418 Donlon, C. J., Martin, M., Stark, J., Roberts-Jones, J., Fiedler, E., and Wimmer, W.: The Operational
419 Sea Surface Temperature and Sea Ice Analysis (OSTIA) system, *Remote Sens. Environ.*, 116,
420 140-158, doi: 10.1016/j.rse.2010.10.017, 2011.
421

422 Fangohr, S., and Woolf, D. K.: Application of new parameterizations of gas transfer velocity and
423 their impact on regional and global marine CO₂ budgets, *J. Marine Syst.*, 66, 195-203,
424 doi:10.1016/j.jmarsys.2006.01.012, 2007.
425

426 Garbe, C. S., Rutgersson, A., Boutin, J., de Leeuw, G., Delille, B., Fairall, C. W., Gruber, N., Hare,
427 J., Ho, D. T., Johnson, M. T., Nightingale, P. D., Pettersson, H., Piskozub, J., Sahlée, E., Tsai, W.,
428 Ward, B., Woolf, D. K., and Zappa, C. J.: Transfer across the air-sea Interface, in: *Ocean-
429 atmosphere interactions of gases and particles*, edited by: Liss, P. S. and Johnson, M. T., *Earth
430 Sys. Sci.*, Springer, Berlin, Heidelberg, 55–111, 2014.
431

432 Goddijn-Murphy, L., Woolf, D. K., Callaghan, A. H.: Parameterizations and algorithms for oceanic
433 whitecap coverage, *J. Phys. Oceanogr.*, 41, 742-756, doi:10.1175/2010JPO4533.1, 2011.
434

435 Goddijn-Murphy, L. M., Woolf, D. K., and Marandino, C.: Space-based retrievals of air-sea gas
436 transfer velocities using altimeters: Calibration for dimethyl sulfide, *J. Geophys. Res.*, 117,
437 C08028, doi: 10.1029/2011JC007535, 2012.
438

439 Goddijn-Murphy, L. M., Woolf, D. K., Land, P. E., Shutler J. D., Donlon, C.: The OceanFlux
440 Greenhouse Gases methodology for deriving a sea surface climatology of CO₂ fugacity in
441 support of air-sea gas flux studies, *Ocean Sci.*, 11, 519-541, doi: 10.5194/os-11-519-2015, 2015.
442

443 Goddijn-Murphy, L., Woolf, D. K., Callaghan, A. H., Nightingale, P. D., and Shutler, J. D.: A
444 reconciliation of empirical and mechanistic models of the air-sea gas transfer velocity, *J.
445 Geophys. Res. Oceans*, 121, 818-835, doi:10.1002/2015JC011096, 2016.
446

447 González-Dávila, M., Santana-Casiano, J. M., and González-Dávila, E. F.: Interannual variability of
448 the upper ocean carbon cycle in the northeast Atlantic Ocean, *Geophys. Res. Lett.*, 34, L07608,
449 doi: 10.1029/2006GL028145, 2007.
450

451 Gregg, W. W., Casey, N. W., Rosseaux, C. S.: Sensitivity of simulated global ocean carbon flux
452 estimates to forcing by reanalysis products, *Ocean Model.*, 80, 24-35, doi:
453 10.1016/j.ocemod.2014.05.002, 2014.
454

455 Gruber, N.: Carbon cycle: Fickle trends in the ocean, *Nature*, 458, 155-156, doi: 10.1038/458155a,
456 2009.
457

458 Halloran, P. R., Booth, B. B. B., Jones, C. D., Lambert, F. H., McNeall, D. J., Totterdell, I. J., and
459 Völker, C.: The mechanisms of North Atlantic CO₂ uptake in a large Earth System Model
460 ensemble, *Biogeosciences*, 12, 4497–4508, doi: 10.5194/bg-12-4497-2015, 2015.
461

462 Ho, D. T., Law, C. S., Smith, M. J., Schlosser, P., Harvey, M., and Hill, P.: Measurements of air-sea
463 gas exchange at high wind speeds in the Southern Ocean: Implications for global
464 parameterizations, *Geophys. Res. Lett.*, 33, 16611, doi: 10.1029/2006/GL026817, 2006.
465

466 Landschützer, P., Gruber, N., Bakker, D. C. E., Schuster, U., Nakaoka, S., Payne, M. R., Sasse, T. P.,
467 and Zeng, J.: A neural network-based estimate of the seasonal to inter-annual variability of the

- 468 Atlantic Ocean carbon sink, *Biogeosciences*, 10, 7793-7815, doi: 10.5194/bg-10-7793-2013,
469 2013.
- 470
- 471 Landschützer, P., Gruber, N., Bakker, D. C. E., Schuster, U.: Recent variability of the global ocean
472 carbon sink, *Global Biogeochem. Cycles*, 28, 927–949, doi: 10.1002/2014GB004853, 2014.
- 473
- 474 Le Quéré, C., Rödenbeck, C., Buitenhuis, E. T., Conway, T. J., Langenfelds, R., Gomez, A.,
475 Labuschagne, C., Ramonet, M., Nakazawa, T., Metzl, N., Gillett, N., Heimann, M.: Saturation of
476 the Southern Ocean CO₂ sink due to recent climate change, *Science* 316, 1735-1738,
477 doi:10.1126/science.1136188, 2007.
- 478
- 479 Le Quéré, C., Moriarty, R., Andrew, R. M., Peters, G. P., Ciais, P., Friedlingstein, P., Jones, S. D.,
480 Sitch, S., Tans, P., Arneeth, A., Boden, T. A., Bopp, L., Bozec, Y., Canadell, J. G., Chini, L. P.,
481 Chevallier, F., Cosca, C. E., Harris, I., Hoppema, M., Houghton, R. A., House, J. I., Jain, A. K.,
482 Johannessen, T., Kato, E., Keeling, R. F., Kitidis, V., Klein Goldewijk, K., Koven, C., Landa, C.
483 S., Landschützer, P., Lenton, A., Lima, I. D., Marland, G., Mathis, J. T., Metzl, N., Nojiri, Y.,
484 Olsen, A., Ono, T., Peng, S., Peters, W., Pfeil, B., Poulter, B., Raupach, M. R., Regnier, P.,
485 Rödenbeck, C., Saito, S., Salisbury, J. E., Schuster, U., Schwinger, J., Séférian, R., Segschneider,
486 J., Steinhoff, T., Stocker, B. D., Sutton, A. J., Takahashi, T., Tilbrook, B., van der Werf, G. R.,
487 Viovy, N., Wang, Y.-P., Wanninkhof, R., Wiltshire, A., and Zeng, N.: Global carbon budget 2014,
488 *Earth Syst. Sci. Data*, 7, 47–85, doi: 10.5194/essd-7-47-2015, 2015.
- 489
- 490 Lefèvre, N., Watson, A. J., Olsen, A., Rios, A. F., Perez, F. F., Johannessen, T.: A decrease in the
491 sink for atmospheric CO₂ in the North Atlantic, *Geophys. Res. Lett.*, 31, L07306, doi:
492 10.1029/2003GL018957, 2004.
- 493
- 494 McGillis, W. R., and Edson, J. B., Hare, J. E., Fairall, C. W.: Direct covariance air-sea CO₂ fluxes,
495 *J. Geophys. Res.*, 106, C8 16729-16745, 2001.
- 496
- 497 Merchant, C. M., Embury, O., Rayner, N. A., Berry, D. I., Corlett, G. K., Lean, K., Veal, K. L., Kent,
498 E. C., Llewellyn-Jones, D. T., Remedios, J. J., and Saunders, R.: A 20 year independent record of
499 sea surface temperature for climate from Along-Track Scanning Radiometers, *J. Geophys. Res.*,
500 117, C12, doi:10.1029/2012JC008400, 2012.
- 501
- 502 Nightingale, P. D., Malin, G., Law, C. S., Watson, A. J., Liss, P. S., Liddicoat, M. I., Boutin, J., and
503 Upstill-Goddard, R. C.: In situ evaluation of air-sea gas exchange parameterizations using novel
504 conservative and volatile tracers, *Global Biogeochem. Cycles*, 14, 373-387, 2000.
- 505
- 506 Nightingale, P. D., Relationship between wind speed and gas exchange over the ocean: which
507 parameterisation should I use? Report from Discussion Session at SOLAS Open Science
508 conference in Kiel, <http://goo.gl/TrMQkg>, 2015.
- 509
- 510 Orr, J. C., Maier-Reimer, E., Mikolajewicz, U., Monfray, P., Sarmiento, J. L., Toggweiler, J. R.,
511 Taylor, N. K., Palmer, J., Gruber, N., Sabine, C. L., Le Quéré, C., Key, R. M., Boutin, J.:
512 Estimates of anthropogenic carbon uptake from four three-dimensional global ocean models,
513 *Global Biogeochem. Cycles*, 15, 43-60, doi: 10.1029/2000GB001273, 2001.
- 514
- 515 Pérez, F. F., Mercier, H., Vázquez-Rodríguez, M., Lherminier, P., Velo, A., Pardo, P. C., Rosón, G.,
516 and Ríos, A. F.: Atlantic Ocean CO₂ uptake reduced by weakening of the meridional overturning
517 circulation, *Nat. Geosci.*, 6, 146-152, doi: 10.1038/NGEO1680, 2013.
- 518
- 519 Pfeil, B., Olsen, A., Bakker, D. C. E., Hankin, S., Koyuk, H., Kozyr, A., Malczyk, J., Manke, A.,

520 Metzl, N., Sabine, C. L., Akl, J., Alin, S. R., Bates, N., Bellerby, R. G. J., Borges, A., Boutin, J.,
521 Brown, P. J., Cai, W.-J., Chavez, F. P., Chen, A., Cosca, C., Fassbender, A. J., Feely, R. A.,
522 González-Dávila, M., Goyet, C., Hales, B., Hardman-Mountford, N., Heinze, C., Hood, M.,
523 Hoppema, M., Hunt, C. W., Hydes, D., Ishii, M., Johannessen, T., Jones, S. D., Key, R. M.,
524 Körtzinger, A., Landschützer, P., Lauvset, S. K., Lefèvre, N., Lenton, A., Lourantou, A.,
525 Merlivat, L., Midorikawa, T., Mintrop, L., Miyazaki, C., Murata, A., Nakadate, A., Nakano, Y.,
526 Nakaoka, S., Nojiri, Y., Omar, A. M., Padin, X. A., Park, G.-H., Paterson, K., Perez, F. F., Pierrot,
527 D., Poisson, A., Ríos, A. F., Santana-Casiano, J. M., Salisbury, J., Sarma, V. V. S. S., Schlitzer,
528 R., Schneider, B., Schuster, U., Sieger, R., Skjelvan, I., Steinhoff, T., Suzuki, T., Takahashi, T.,
529 Tedesco, K., Telszewski, M., Thomas, H., Tilbrook, B., Tjiputra, J., Vandemark, D., Veness, T.,
530 Wanninkhof, R., Watson, A. J., Weiss, R., Wong, C. S., and Yoshikawa-Inoue, H.: A uniform,
531 quality controlled Surface Ocean CO₂ Atlas (SOCAT), *Earth Syst. Sci. Data*, 5, 125-143, doi:
532 10.5194/essd-5-125-2013, 2013.

533

534 Sabine, C. L., Hankin, S., Koyuk, H., Bakker, D. C. E., Pfeil, B., Olsen, A., Metzl, N., Kozyr, A.,
535 Fassbender, A., Manke, A., Malczyk, J., Akl, J., Alin, S. R., Bellerby, R. G. J., Borges, A.,
536 Boutin, J., Brown, P. J., Cai, W.-J., Chavez, F. P., Chen, A., Cosca, C., Feely, R. A., González-
537 Dávila, M., Goyet, C., Hardman-Mountford, N., Heinze, C., Hoppema, M., Hunt, C. W., Hydes,
538 D., Ishii, M., Johannessen, T., Key, R. M., Körtzinger, A., Landschützer, P., Lauvset, S. K.,
539 Lefèvre, N., Lenton, A., Lourantou, A., Merlivat, L., Midorikawa, T., Mintrop, L., Miyazaki, C.,
540 Murata, A., Nakadate, A., Nakano, Y., Nakaoka, S., Nojiri, Y., Omar, A. M., Padin, X. A., Park,
541 G.-H., Paterson, K., Perez, F. F., Pierrot, D., Poisson, A., Ríos, A. F., Salisbury, J., Santana-
542 Casiano, J. M., Sarma, V. V. S. S., Schlitzer, R., Schneider, B., Schuster, U., Sieger, R., Skjelvan,
543 I., Steinhoff, T., Suzuki, T., Takahashi, T., Tedesco, K., Telszewski, M., Thomas, H., Tilbrook, B.,
544 Vandemark, D., Veness, T., Watson, A. J., Weiss, R., Wong, C. S., and Yoshikawa-Inoue, H.:
545 Surface Ocean CO₂ Atlas (SOCAT) gridded data products, *Earth Syst. Sci. Data*, 5, 145-153, doi:
546 10.5194/essd-5-145-2013, 2013.

547

548 Schuster, U., and Watson, A. J.: A variable and decreasing sink for atmospheric CO₂ in the North
549 Atlantic, *J. Geophys. Res.*, 112, C11006, doi: 10.1029/2006JC003941, 2007.

550

551 Schuster, U., McKinley, G. A., Bates, N., Chevallier, F., Doney, S. C., Fay, A. R., González-Dávila,
552 M., Gruber, N., Jones, S., Krijnen, J., Landschützer, P., Lefèvre, N., Manizza, M., Mathis, J.,
553 Metzl, N., Olsen, A., Ríos, A. F., Rödenbeck, C., Santana-Casiano, J. M., Takahashi, T.,
554 Wanninkhof, R., and Watson, A. J.: An assessment of the Atlantic and Arctic sea-air CO₂ fluxes,
555 1990–2009, *Biogeosciences*, 10, 607–627, doi: 10.5194/bg-10-607-2013, 2013.

556

557 Shutler, J. D., Piolle, J-F., Land, P. E., Woolf, D. K., Goddijn-Murphy, L., Paul, F., Girard-Arduin,
558 F., Chapron, B., and Donlon, C. J.: FluxEngine: a flexible processing system for calculating air-
559 sea carbon dioxide gas fluxes and climatologies, *J. Atmos. Ocean. Tech.*, doi:10.1175/JTECH-D-
560 14-00204.1, 2016.

561

562 Sweeney, C., Gloor, E., Jacobson, A. R., Key, R. M., McKinley, G., Sarmiento, J. L., and
563 Wanninkhof, R.: Constraining global air-sea gas exchange for CO₂ with recent bomb 14C
564 measurements, *Global Biogeochem. Cycles*, 21, doi:10.1029/2006GB002784, 2007.

565

566 Takahashi, T., Sutherland, S. C., Sweeney, C., Poisson, A., Metzl, N., Tilbrook, B., Bates, N.,
567 Wanninkhof, R., Feely, R. A., Sabine, C., Olafsson, J., and Nojiri, Y.: Global sea-air CO₂ flux
568 based on climatological surface ocean pCO₂, and seasonal biological and temperature effects,
569 *Deep-Sea Res., Pt. II*, 49, 1601-1622, 2002.

570

571 Takahashi, T., Sutherland, S. C., Wanninkhof, R., Sweeney, C., Feely, R. A., Chipman, D. W., Hales,

572 B., Friederich, G., Chavez, F., Sabine, C., Watson, A., Bakker, D. C. E., Schuster, U., Metzl, N.,
573 Yoshikawa-Inoue, H., Ishii, M., Midorikawa, T., Nojiri, Y., Körtzinger, A., Steinhoff, T.,
574 Hoppema, M., Olafsson, J., Arnarson, T. S., Tilbrook, B., Johannessen, T., Olsen, A., Bellerby,
575 R., Wong, C. S., Delille, B., Bates, N. R., and de Baar, H. J. W.: Climatological mean and
576 decadal change in surface ocean $p\text{CO}_2$ and net sea-air CO_2 flux over the global oceans, *Deep-Sea*
577 *Res. Pt. II*, 56, 554–577, doi: 10.1016/j.dsr2.2008.12.009, 2009.

578

579 Talley, L. D.: Closure of the global overturning circulation through the Indian, Pacific, and Southern
580 Oceans: schematics and transports, *Oceanography* 26(1), 80–97, doi:10.5670/oceanog.2013.07,
581 2013.

582

583 Thomas, H., Friederike Prowe, A. E., Lima, I. D., Doney, S. C., Wanninkhof, R., Greatbatch, R. J.,
584 Schuster, U., and Corbière, A.: Changes in the North Atlantic Oscillation influence CO_2 uptake
585 in the North Atlantic over the past 2 decades, *Global Biogeochem. Cycles*, 22, GB4027,
586 doi:10.1029/2007GB003167, 2008.

587

588 Wanninkhof, R.: Relationship between wind speed and gas exchange over the ocean revisited,
589 *Limnol. Oceanogr. Methods*, 12, 351–362, doi: 10.4319/lom.2014.12.351, 2014.

590

591 Wanninkhof, R., and McGillis, W. R.: A cubic relationship between air-sea CO_2 exchange and wind
592 speed, *Geophys. Res. Lett.*, 26, 1889–1892, 1999.

593

594 Wanninkhof, R., Park, G.-H., Takahashi, T., Sweeney, C., Feely, R., Nojiri, Y., Gruber, N., Doney, S.
595 C., McKinley, G. A., Lenton, A., Le Quéré, C., Heinze, C., Schwinger, J., Graven, H.,
596 Khatiwala, S.: Global ocean carbon uptake: magnitude, variability and trends, *Biogeosciences*,
597 10, 1983–2000, doi: 10.5194/bg-10-1983-2013, 2013.

598

599 Watson, A. J., Schuster, U., Bakker, D. C. E., Bates, N. R., Corbière, A., González-Dávila, M.,
600 Friedrich, T., Hauck, J., Heinze, C., Johannessen, T., Körtzinger, A., Metzl, N., Olafsson, J.,
601 Olsen, A., Oschlies, A., Padin, X. A., Pfeil, B., Santana-Casiano, J. M., Steinhoff, T., Telszewski,
602 M., Rios, A. F., Wallace, D. W., Wanninkhof, R.: Tracking the variable North Atlantic sink for
603 atmospheric CO_2 , *Science*, 326(5958), 1391–1393, doi: 10.1126/science.1177394, 2009.

604

605 Watson, A. J., Metzl, N., Schuster, U.: Monitoring and interpreting the ocean uptake of atmospheric
606 CO_2 , *Philos. T. R. Soc. A*, 369, 1997–2008, doi: 10.1098/rsta.2011.0060, 2011.

607

608 Woolf, D. K.: Parameterization of gas transfer velocities and sea-state dependent wave breaking.
609 *Tellus B*, 57, 87–94, 2005.

610

611 Woolf, D. K., Shutler, J. D., Goddijn-Murphy, L., Donlon, C. J., Nightingale, P. D., Land, P. E.,
612 Torres, R., Chapron, B., Piolle, J-F., Herledan, S., Hanafin, J., Girard-Ardhuin, F., Ardhuin, F.,
613 Prytherch, J., Moat, B., and Yelland, M.: Key uncertainties in the contemporary air-sea flux of
614 carbon dioxide: an OceanFlux study, submitted 2015a.

615

616 Woolf, D. K., Goddijn-Murphy, L. M., Shutler, J. D., Land, P. E., Donlon, C. J., Prytherch, J.,
617 Yelland, M. J., Nightingale, P. D., Torres, R., Chapron, B., Piolle, J-F., Herledan, S., Hanafin, J.,
618 Girard-Ardhuin, F., Ardhuin F., and Moat, B.: Sources and types of uncertainty in the
619 contemporary air-sea flux of carbon dioxide: an OceanFlux study, submitted 2015b.

620

621 Yasunaka, S., Murata, A., Watanabe, E., Chierici, M., Fransson, A., van Heuven, S., Hoppema, M.,
622 Ishii, M., Johannessen, T., Kosugi, N., Lauvset, S. K., Mathis, J. T., Nishino, S., Omar, A. M.,
623 Olsen, A., Sasano, D., Takahashi, T., Wanninkhof, R.: Mapping of the air–sea CO_2 flux in the

624 Arctic Ocean and its adjacent seas: Basin-wide distribution and seasonal to interannual
625 variability, *Polar Sci.*, doi:10.1016/j.polar.2016.03.006, 2016.

626 Figure 1. Seasonal and annual mean air-sea fluxes of CO₂ (mg C m⁻² day⁻¹) in the North Atlantic,
627 using Nightingale et al. (2000) *k* parameterization and Takahashi et al. (2009) climatology a)
628 annual, b) DJF (winter), c) MAM (spring), d) JJA (summer), e) SON (autumn). The gaps (white
629 areas) are due to missing data, land and ice masks.

630
631 Figure 2. Surface ocean currents in the Arctic (sources:
632 http://www.grida.no/graphicslib/detail/ocean-currents-and-sea-ice-extent_4aa6, author: Philippe
633 Rekacewicz, UNEP-GRID, Arendal, Norway). North Atlantic Drift forming the Norwegian Atlantic
634 Current in the Arctic Ocean.

635
636 Figure 3. Seasonal and annual *p*CO₂ values (µatm) in surface waters of the North Atlantic,
637 estimated using the Takahashi et al. (2009) climatology a) annual, b) DJF (winter), c) MAM
638 (spring), d) JJA (summer), e) SON (autumn). The gaps (white areas) are due to missing data, land
639 and ice masks.

640
641 Figure 4. Wind speed distribution *U*₁₀ (ms⁻¹) in the North Atlantic used to determine the relationship
642 between gas transfer velocity and air-sea CO₂ fluxes a) annual, b) DJF (winter), c) MAM (spring),
643 d) JJA (summer), e) SON (autumn). The gaps (white areas) are due to missing data, land and ice
644 masks.

645
646 Figure 5. Differences maps for the air-sea CO₂ fluxes (mg C m⁻² day⁻¹) in the North Atlantic,
647 between a cubed and a squared parameterization (Wanninkhof and McGillis 1999 and Wanninkhof
648 2014) a) annual, b) DJF (winter), c) MAM (spring), d) JJA (summer) e) SON (autumn). The gaps
649 (white areas) are due to missing data, land and ice masks.

650
651 Figure 6. Monthly values of CO₂ air-sea fluxes (Pg month⁻¹) for the five parameterizations (eq. 4-8)
652 a) the North Atlantic, b) the European Arctic.

653
654 Figure 7. Annual air-sea fluxes of CO₂ for the five (eq. 4-8) parameterizations as well as for
655 backscatter (default) and wind driven OceanFlux GHG parameterizations normalized to flux values
656 of Nightingale et al. (2000) *k* parameterization (see text) a) globally, b) the North Atlantic c) the
657 European Arctic, d) the Southern Ocean. Average values for all parameterization and standard
658 deviations are marked as vertical gray lines.

659
660 Figure 8. Comparison of monthly air-sea CO₂ fluxes calculated with different *p*CO₂ datasets
661 (Takahashi et al., 2009, SOCAT v. 1.5 and 2.0) using the same *k* parameterization (Nightingale et
662 al., 2000) a) the North Atlantic, b) the European Arctic.

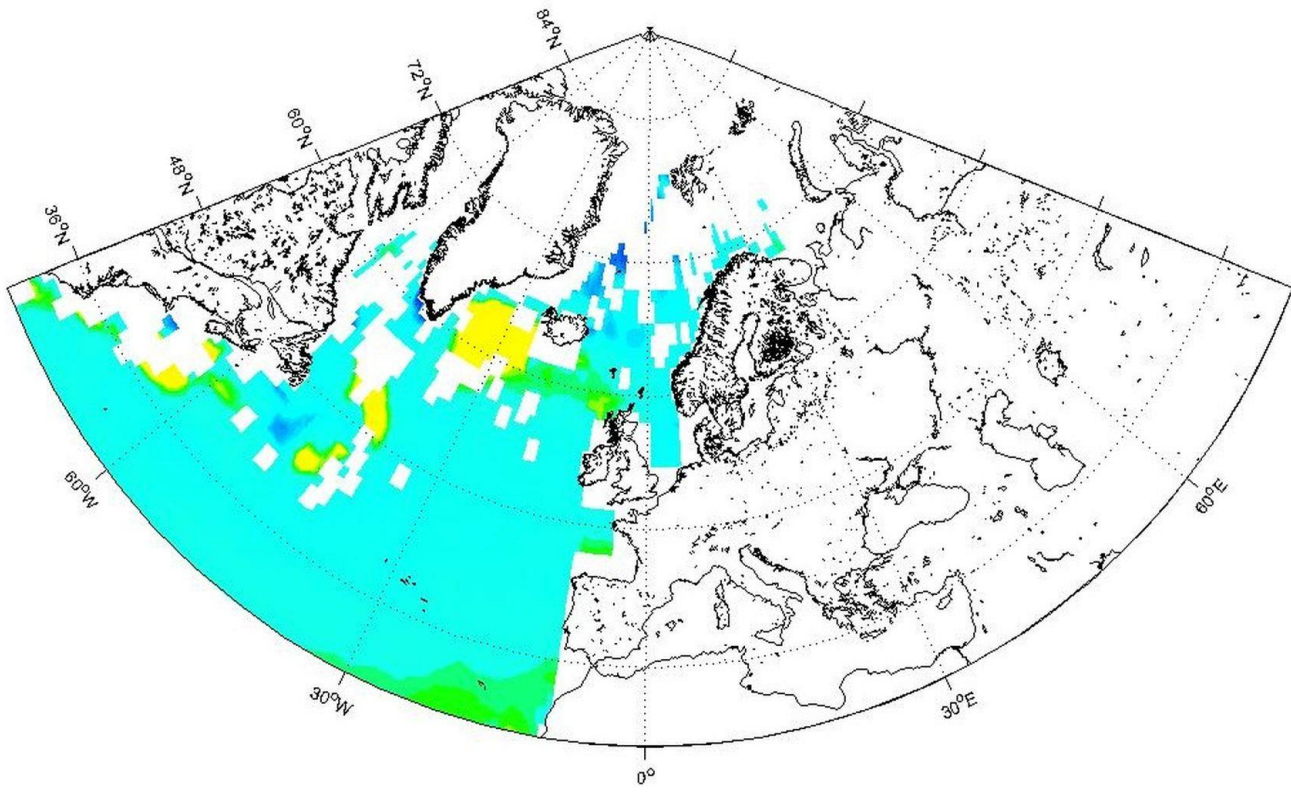
663
664 Figure 9. Different *k* parameterizations as a function of wind speed.

665

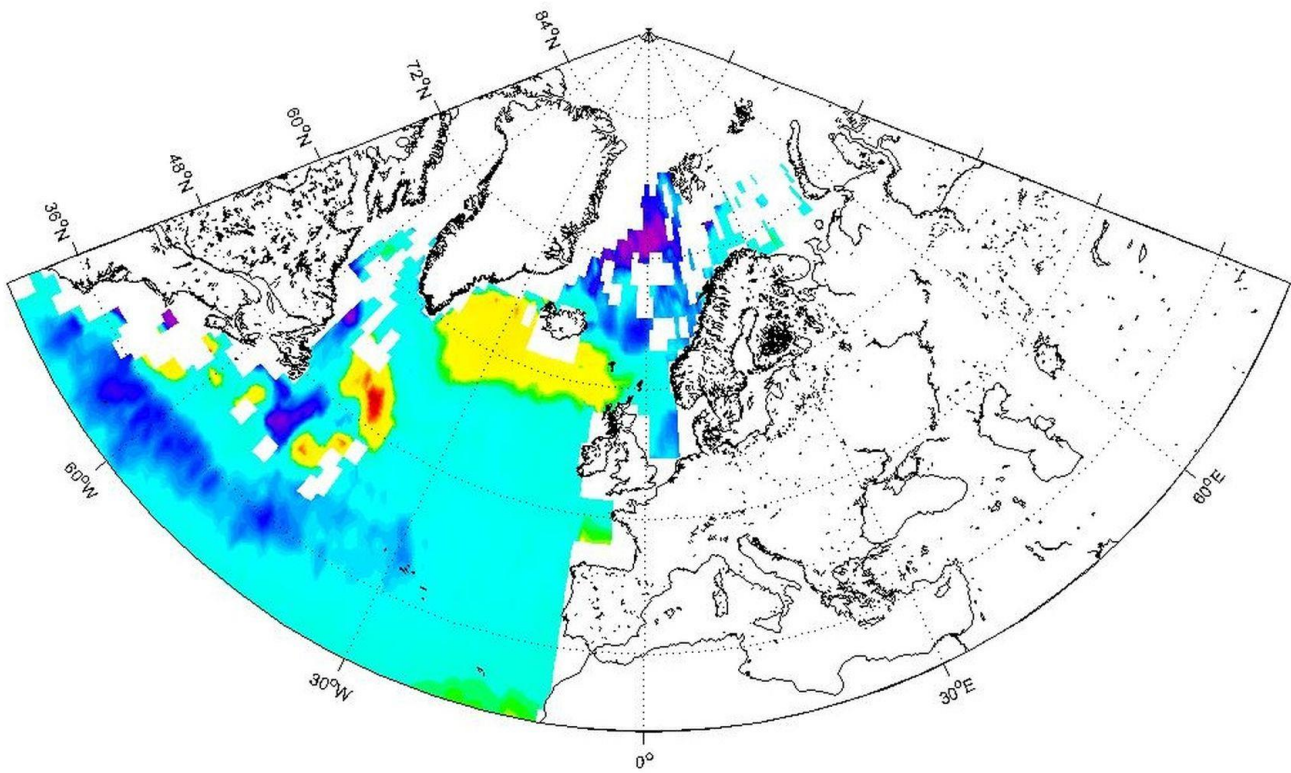
Table 1. Annual air-sea CO₂ fluxes (in Pg) using different k parameterizations. The values in parentheses are fluxes normalized to Nightingale et al., 2000 (as in Fig. 7)

	Global	Arctic	North Atlantic	Southern Ocean
Nightingale et al., 2000	-1.30 (1.00)	-0.102 (1.00)	-0.382 (1.00)	-0.72 (1.00)
Ho et al., 2006	-1.42 (1.09)	-0.106 (1.04)	-0.402 (1.05)	-0.76 (1.06)
Wanninkhof and McGillis, 1999	-1.73 (1.33)	-0.130 (1.28)	-0.490 (1.29)	-0.93 (1.30)
Wanninkhof, 2014	-1.40 (1.08)	-0.105 (1.03)	-0.398 (1.04)	-0.76 (1.05)
McGillis et al., 2001	-2.15 (1.65)	-0.147 (1.44)	-0.557 (1.46)	-1.08 (1.49)
OceanFlux GHG wind driven	-1.98 (1.52)	-0.138 (1.36)	-0.560 (1.47)	-1.14 (1.58)
OceanFluxGHG backscatter	-1.88 (1.44)	-0.130 (1.27)	-0.526 (1.38)	-1.09 (1.51)

669
670 a)



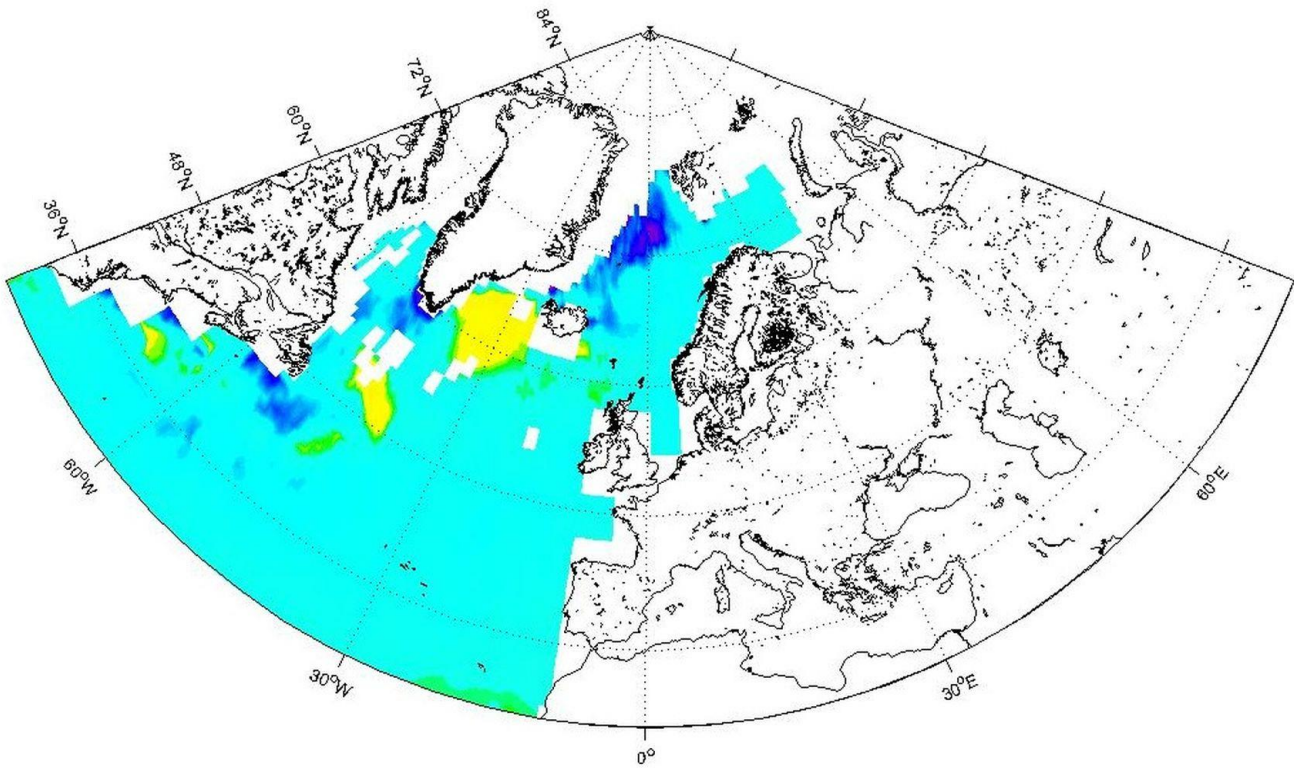
671
672 b)



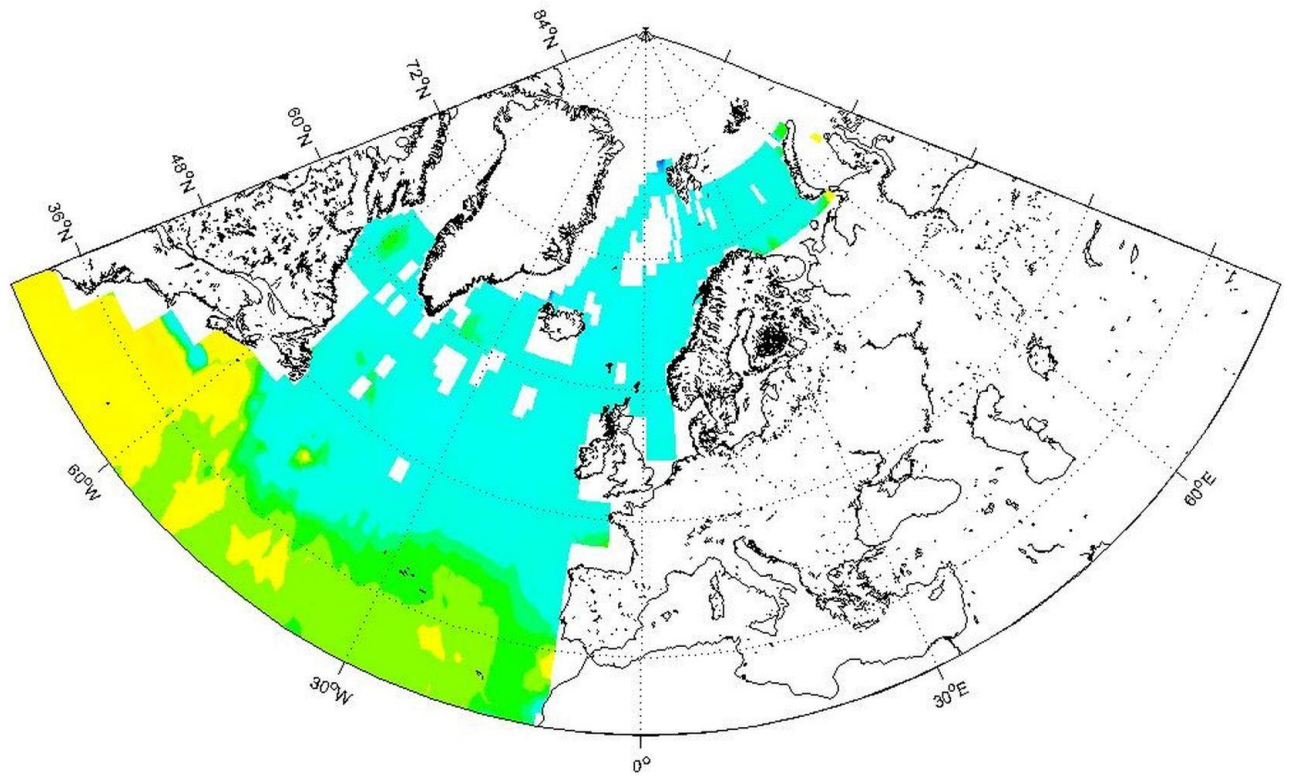
673
674
675

(mg C m⁻² day⁻¹)

676
677 c)



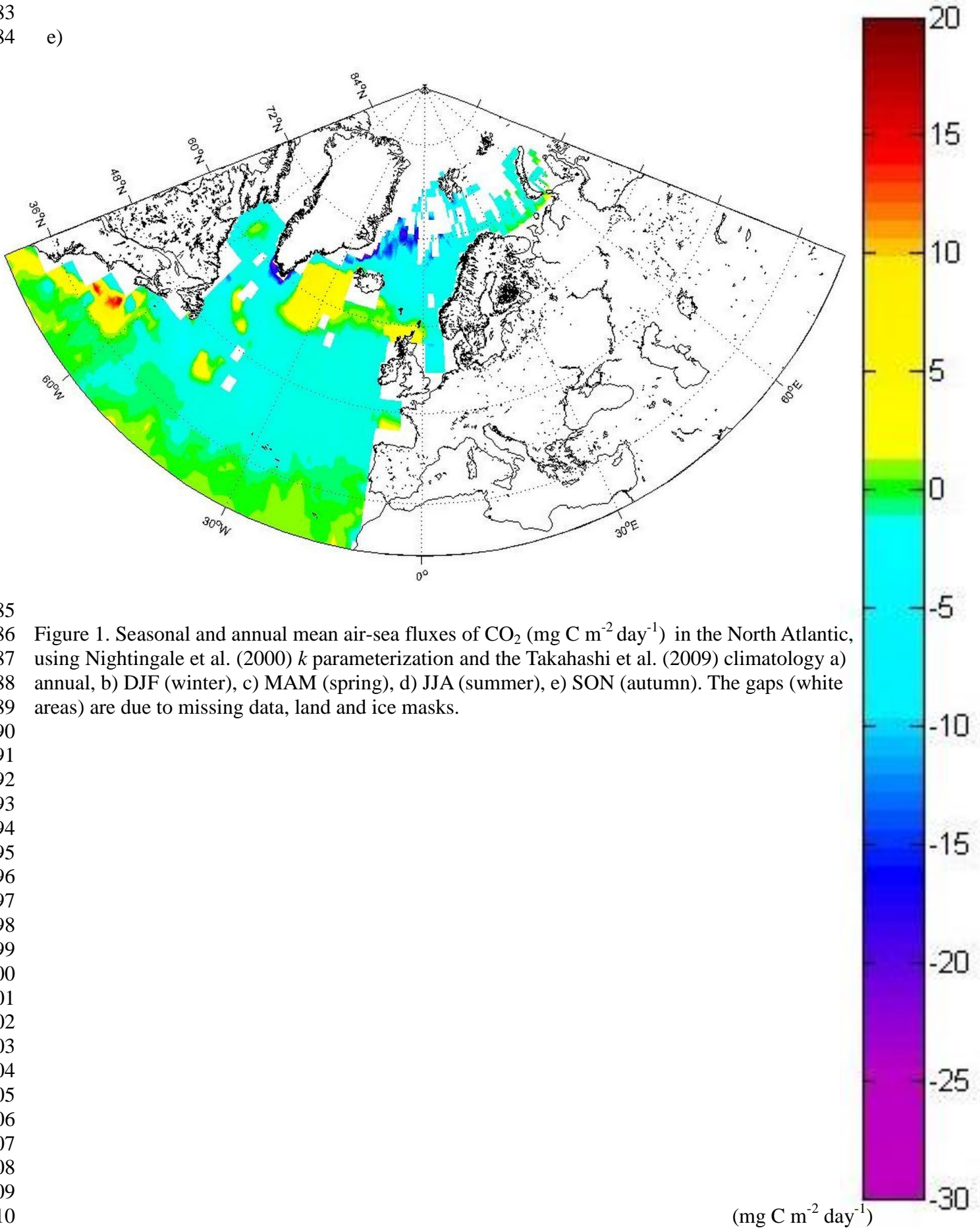
678
679 d)



680
681
682

$(\text{mg C m}^{-2} \text{ day}^{-1})$

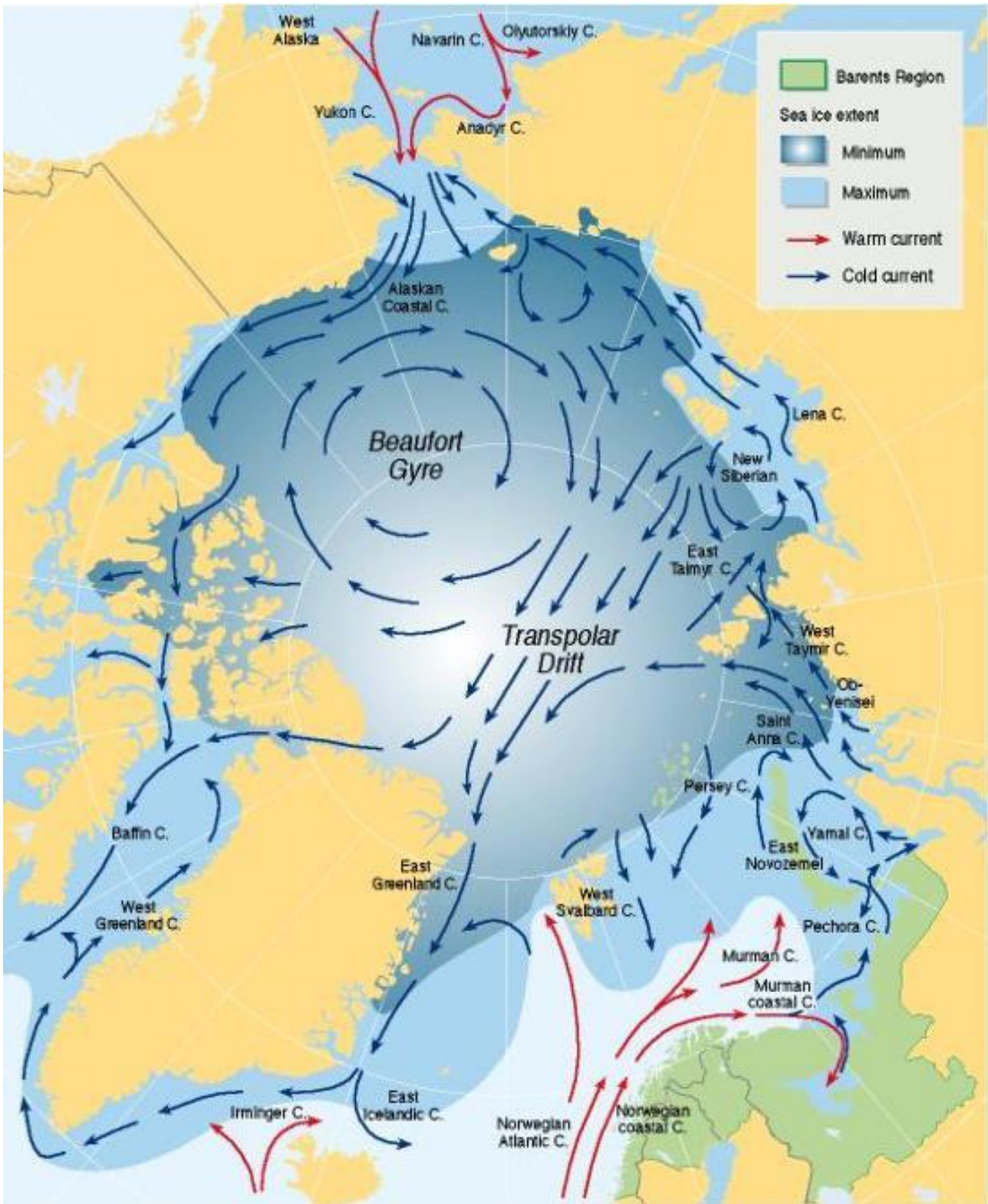
683
684 e)



685
686 Figure 1. Seasonal and annual mean air-sea fluxes of CO₂ (mg C m⁻² day⁻¹) in the North Atlantic,
687 using Nightingale et al. (2000) *k* parameterization and the Takahashi et al. (2009) climatology a)
688 annual, b) DJF (winter), c) MAM (spring), d) JJA (summer), e) SON (autumn). The gaps (white
689 areas) are due to missing data, land and ice masks.

690
691
692
693
694
695
696
697
698
699
700
701
702
703
704
705
706
707
708
709
710
711

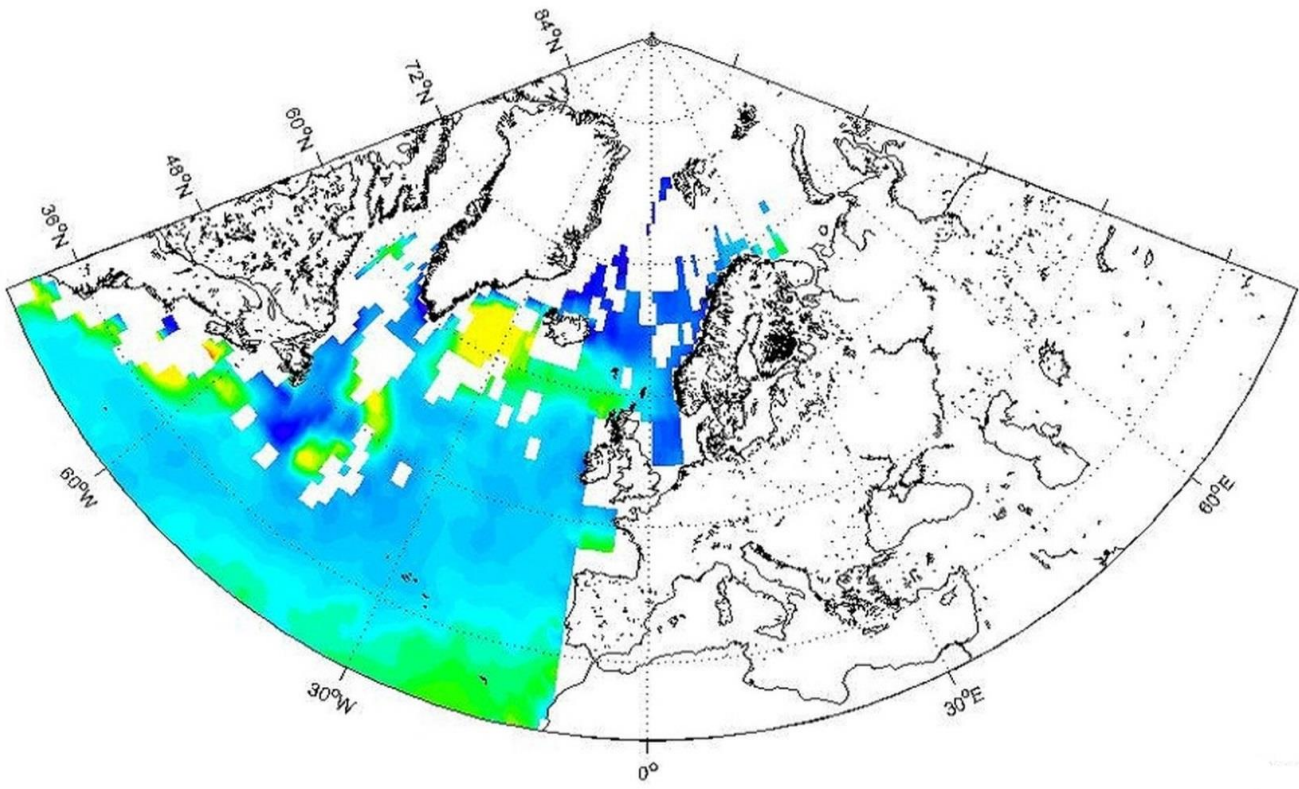
712
713



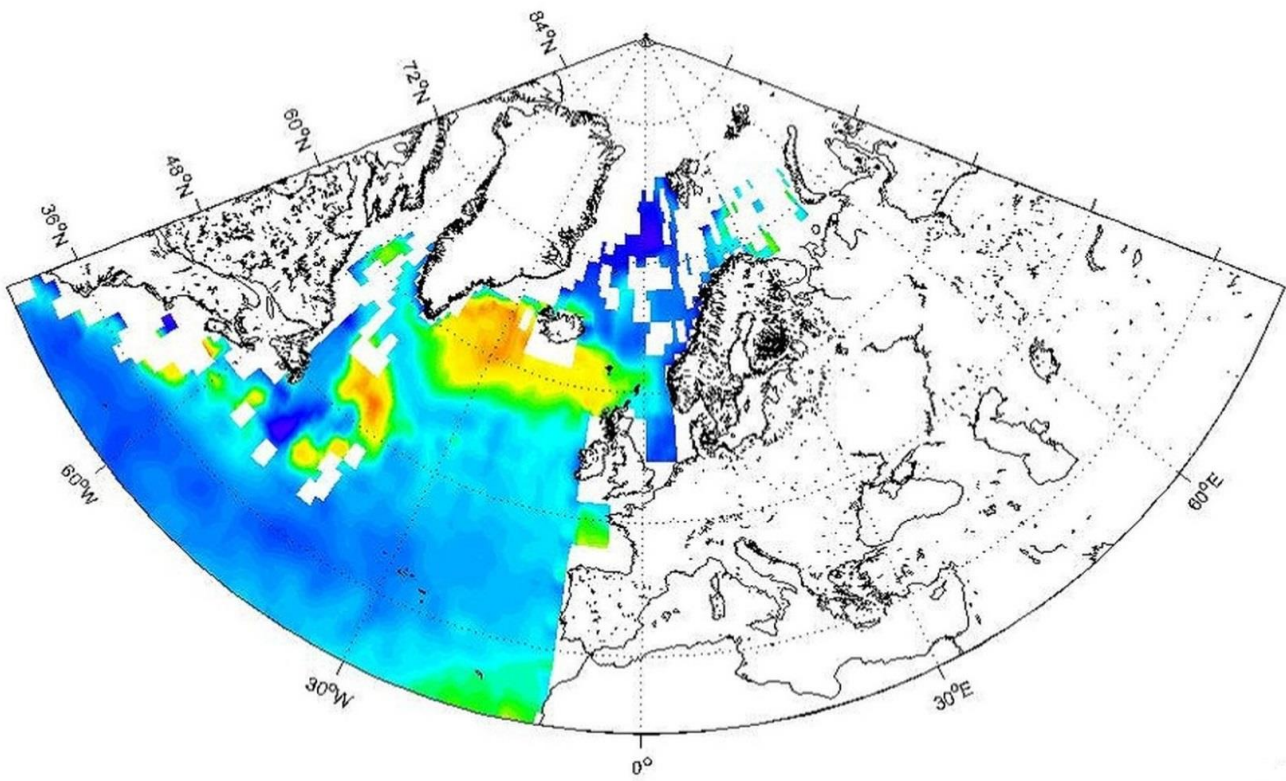
714
715
716
717
718
719

Figure 2. Surface ocean currents in the Arctic (sources: http://www.grida.no/graphicslib/detail/ocean-currents-and-sea-ice-extent_4aa6, author: Philippe Rekacewicz, UNEP-GRID, Arendal, Norway). North Atlantic Drift forming the Norwegian Atlantic Current in the Arctic Ocean.

720
721 a)



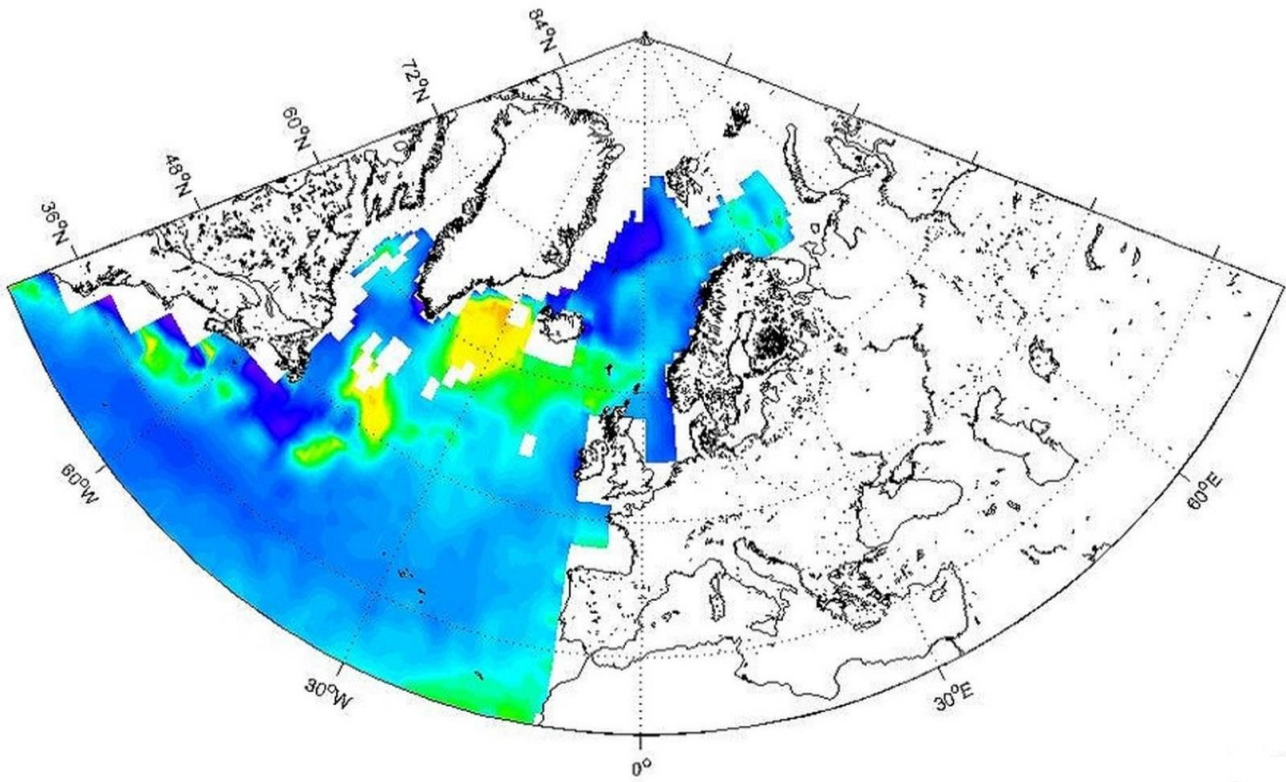
722
723 b)



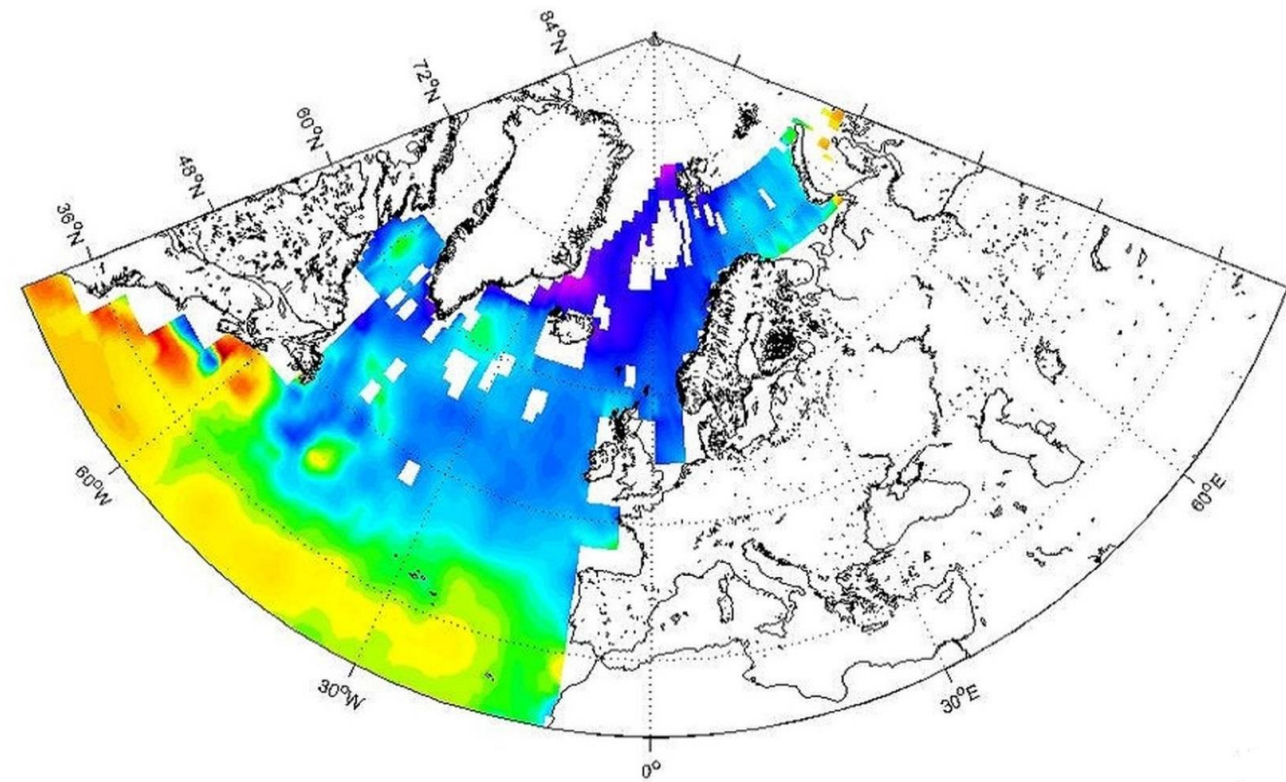
724
725
726

(μatm)

727
728 c)



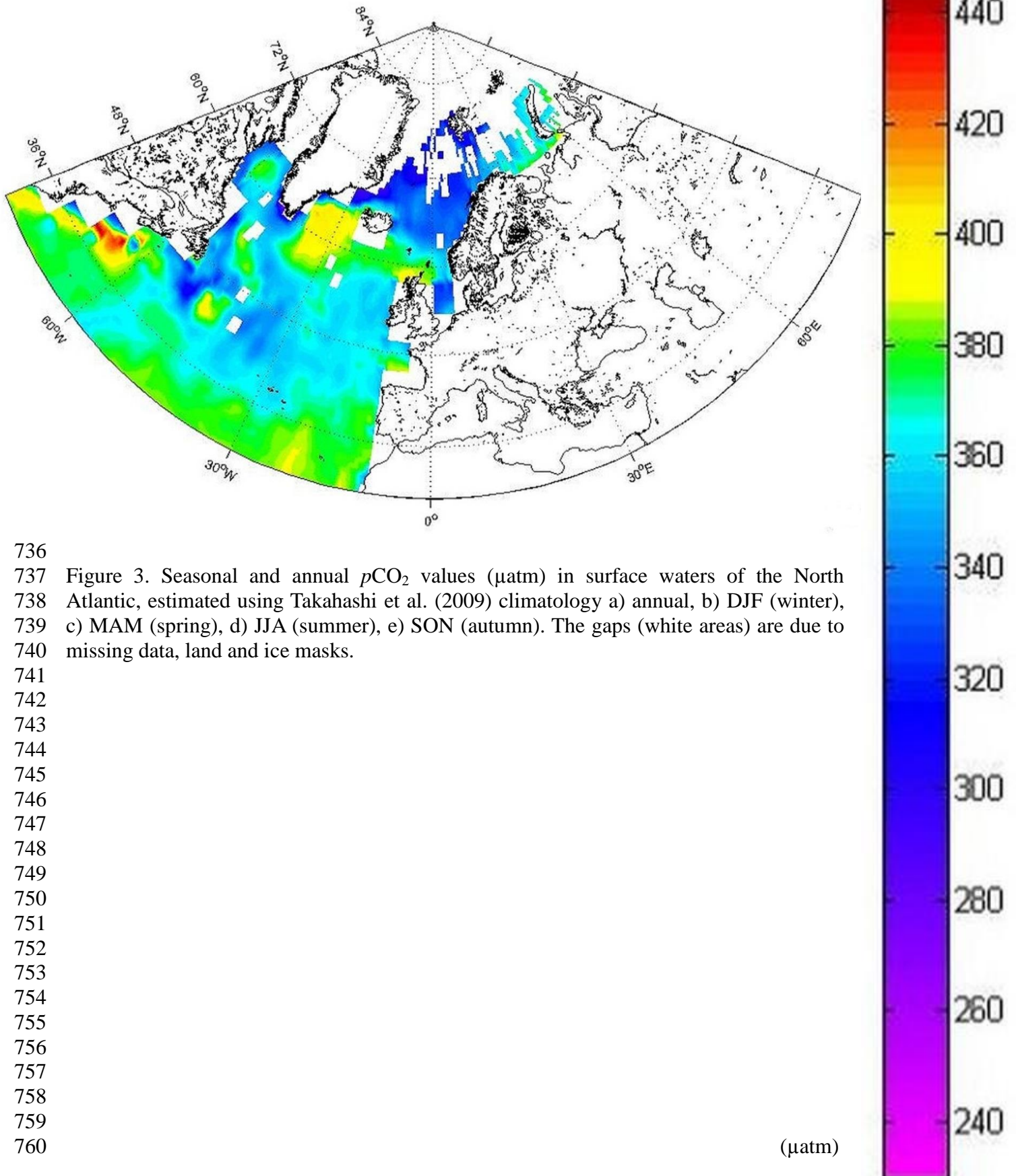
729
730 d)



731
732
733

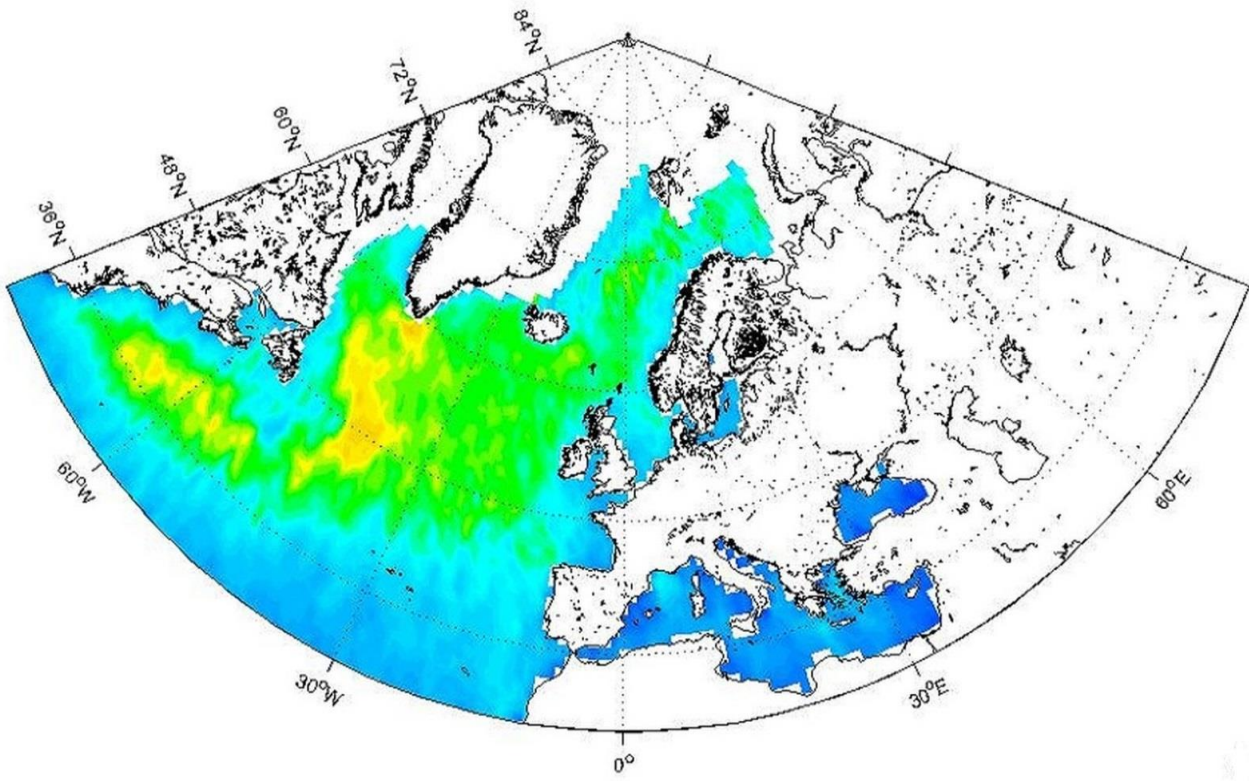
(μatm)

734
735 e)

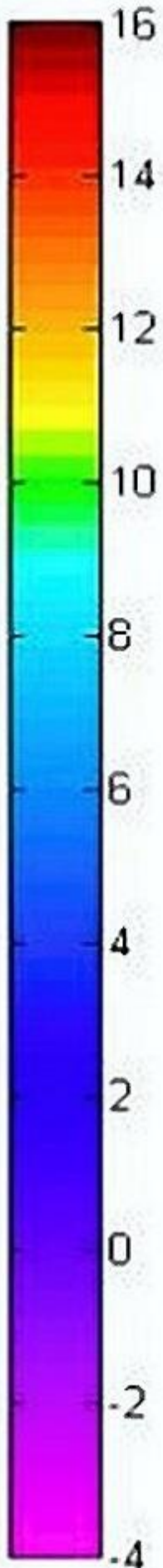
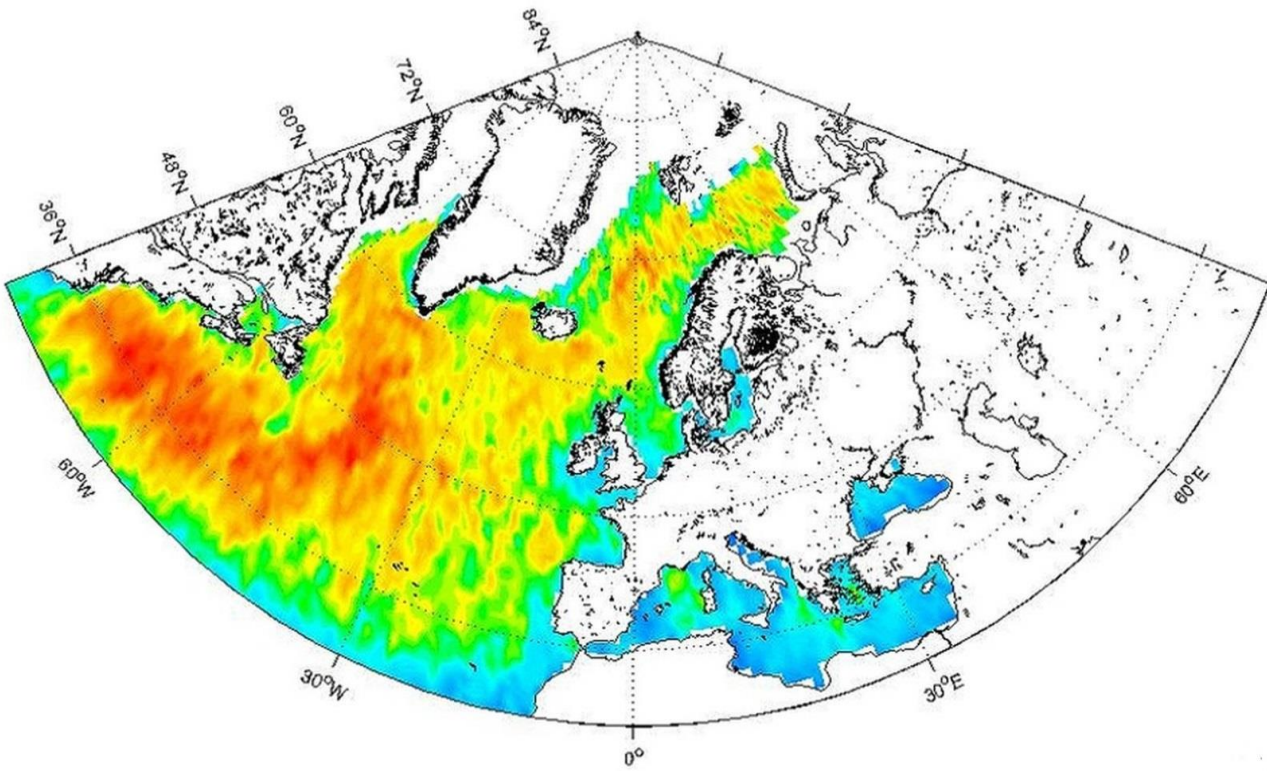


736
737
738
739
740
741
742
743
744
745
746
747
748
749
750
751
752
753
754
755
756
757
758
759
760

761
762 a)



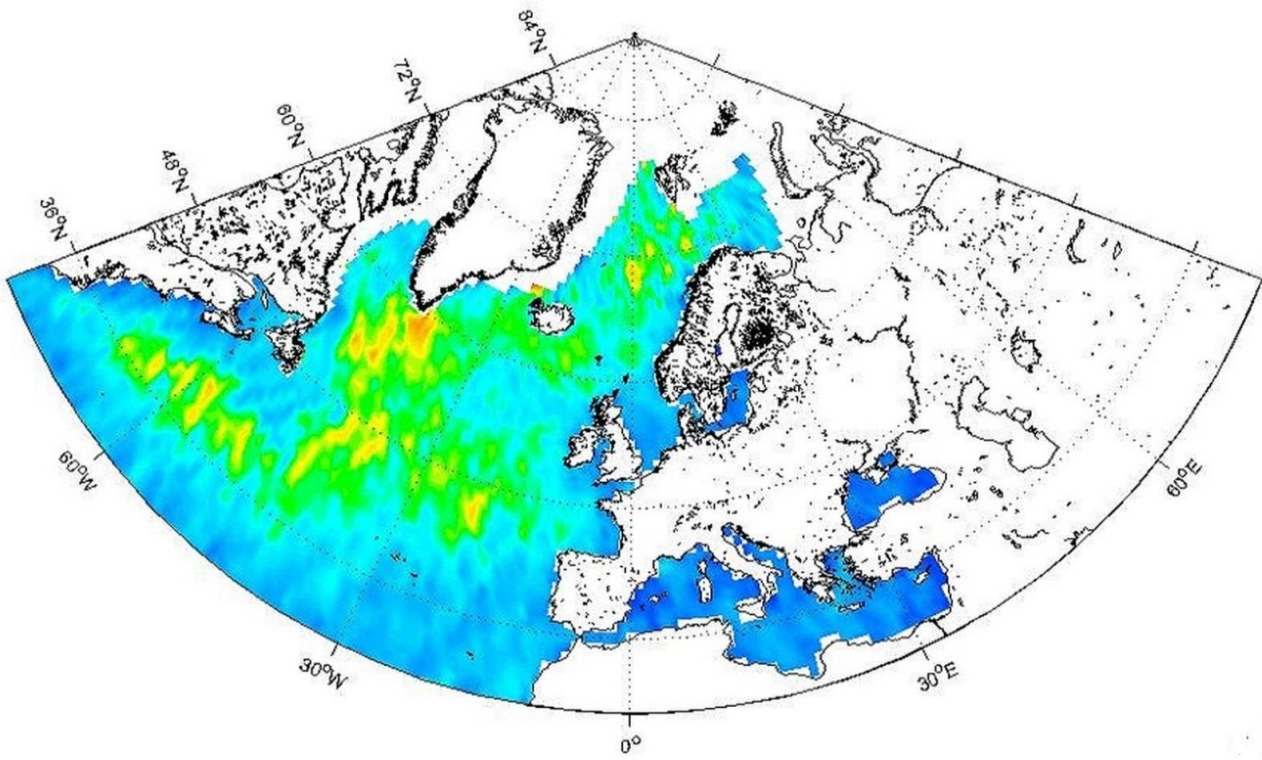
763
764 b)



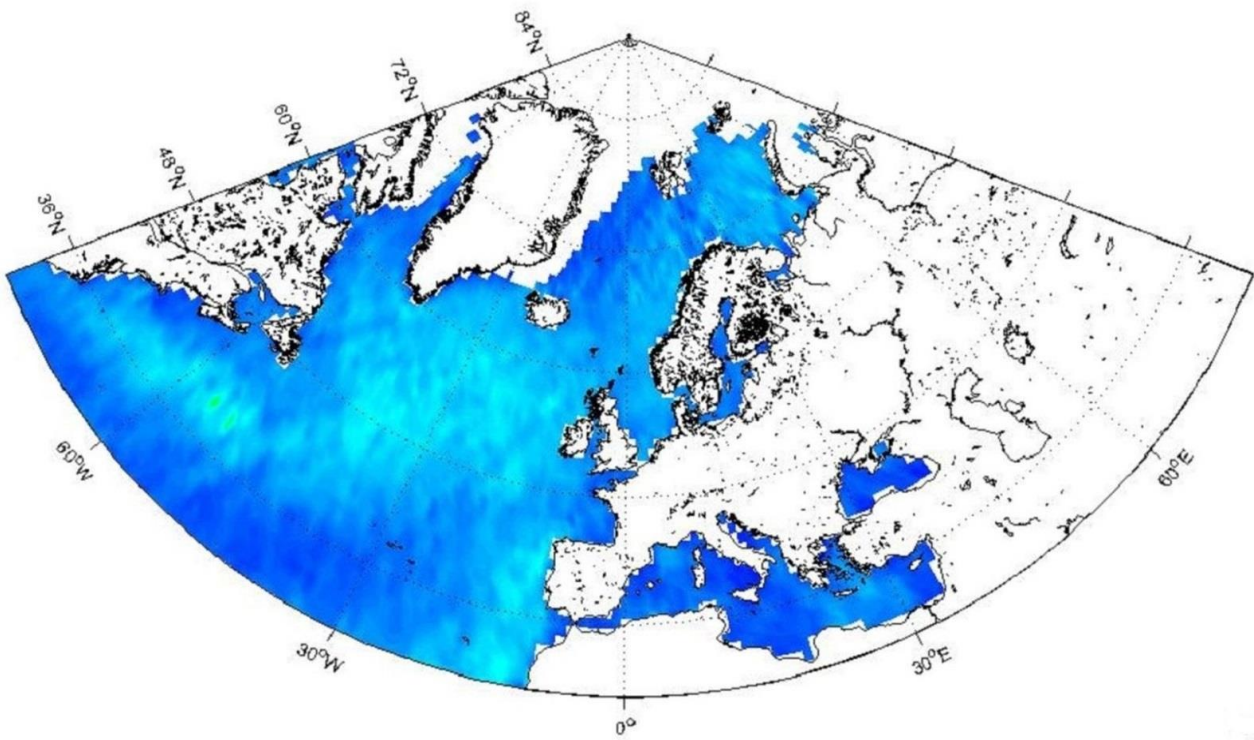
765
766

(ms⁻¹)

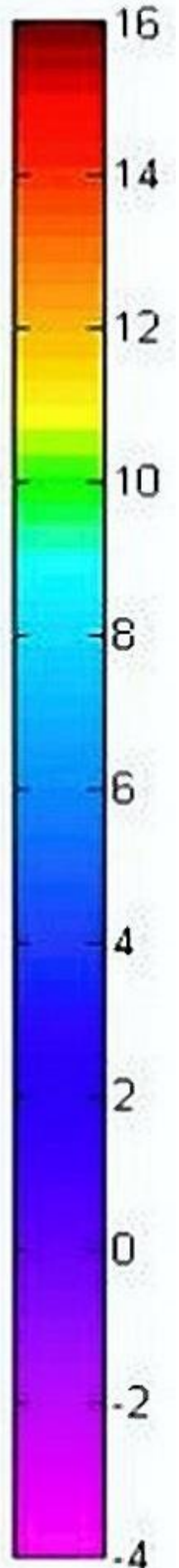
767
768 c)



769
770
771 d)

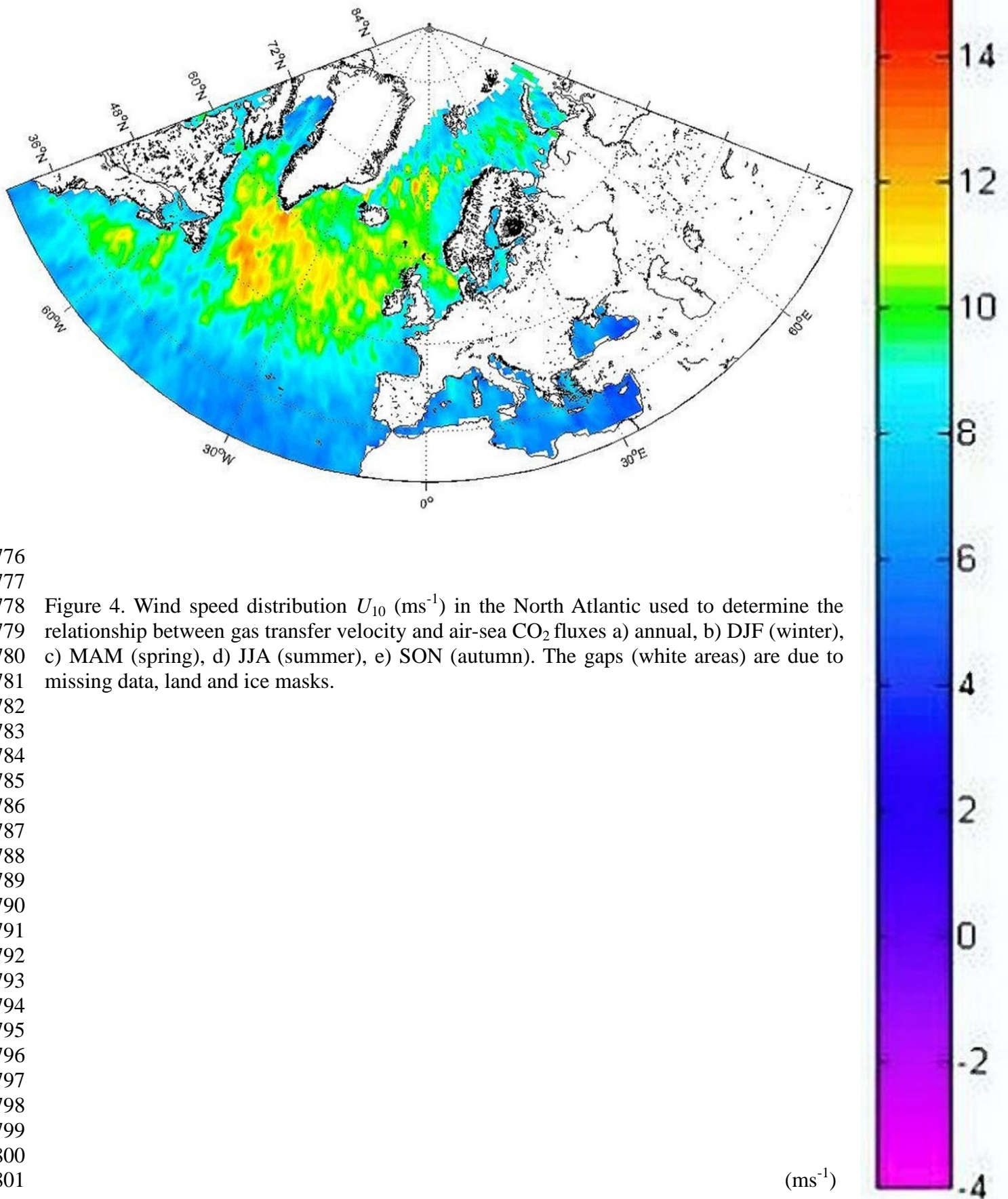


772
773

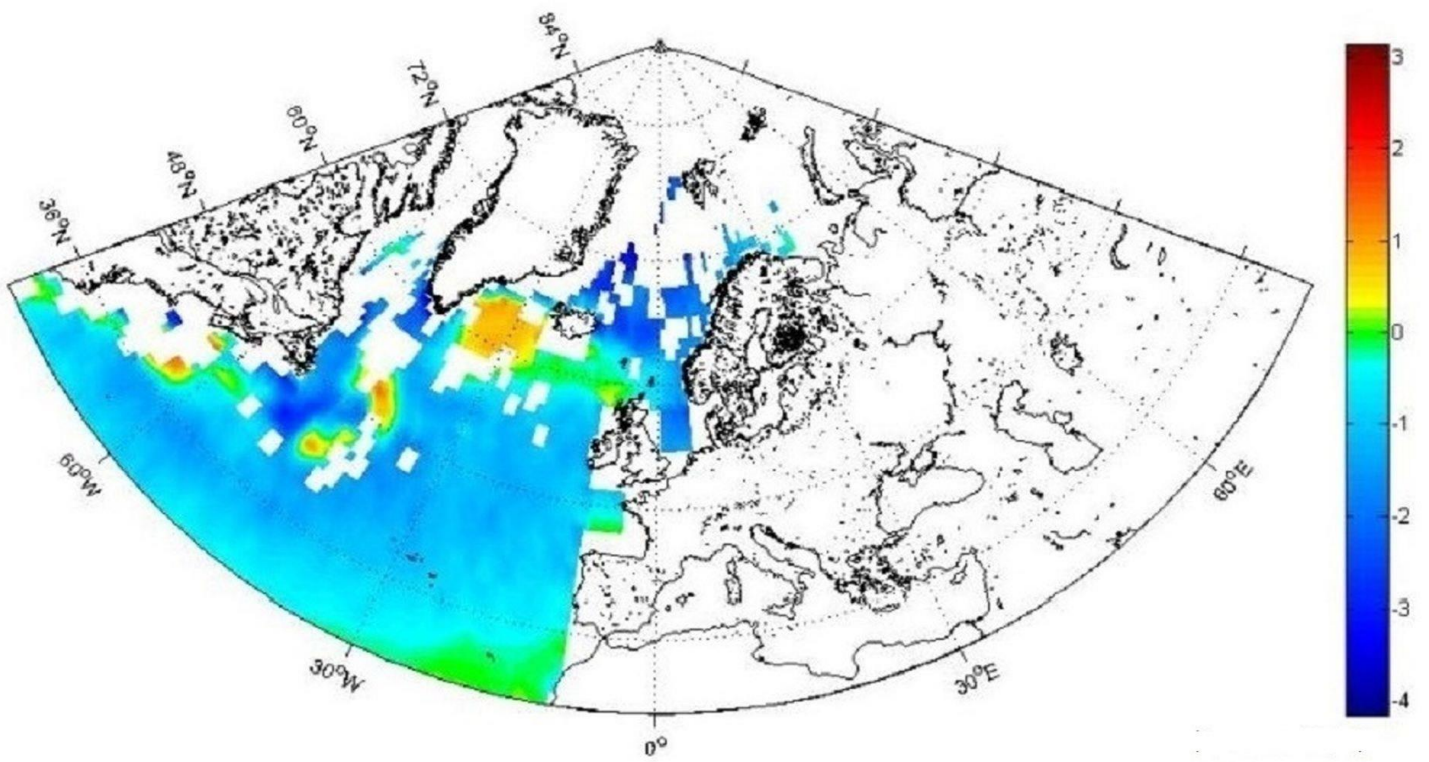


(ms⁻¹)

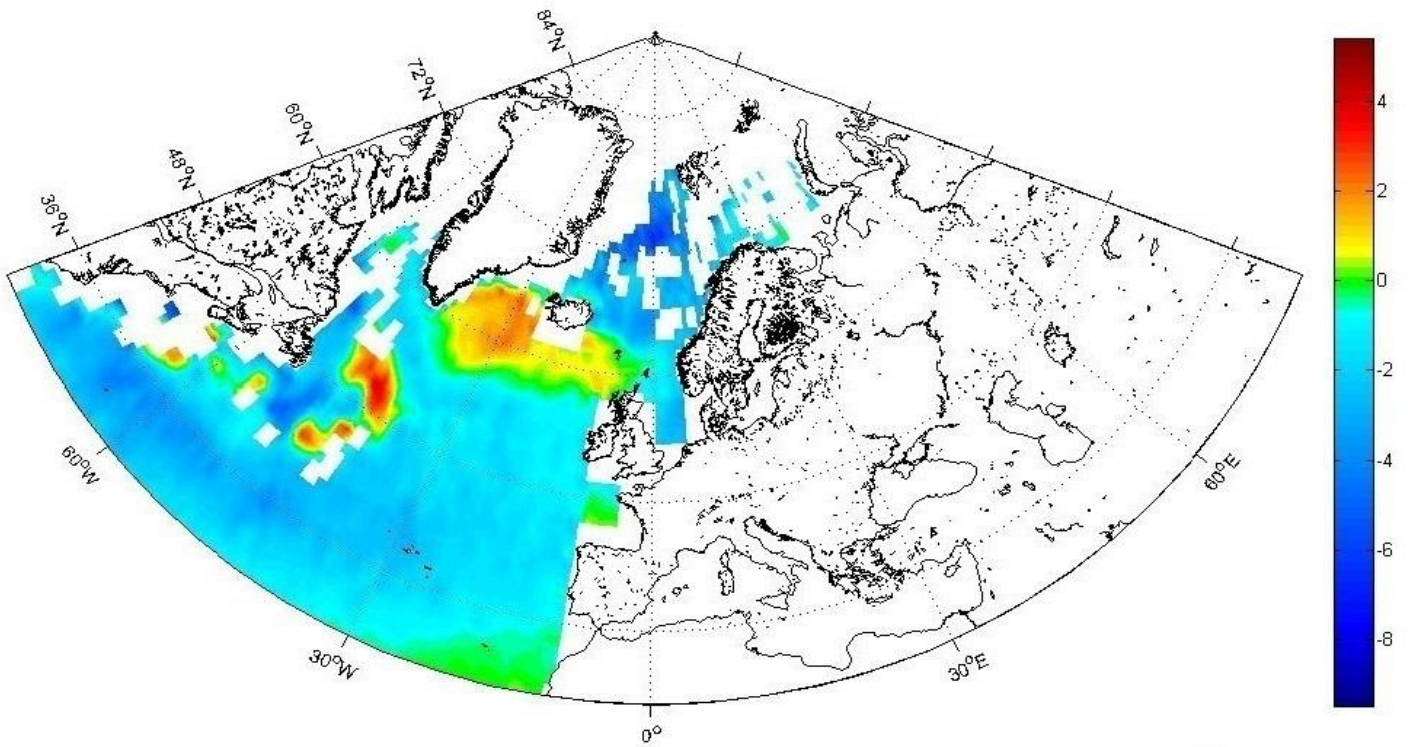
774
775 e)



802
803 a)

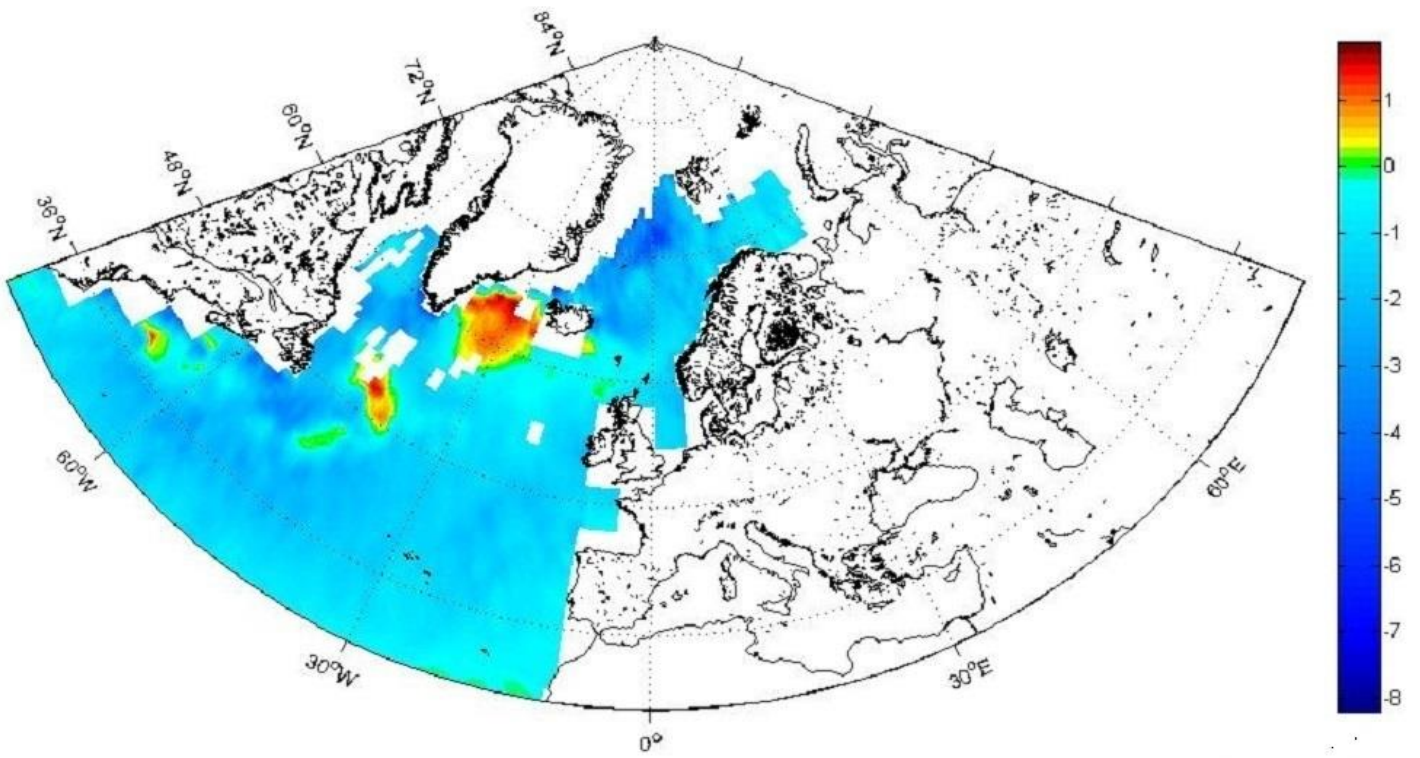


804 (mg C m⁻² day⁻¹)
805 b)



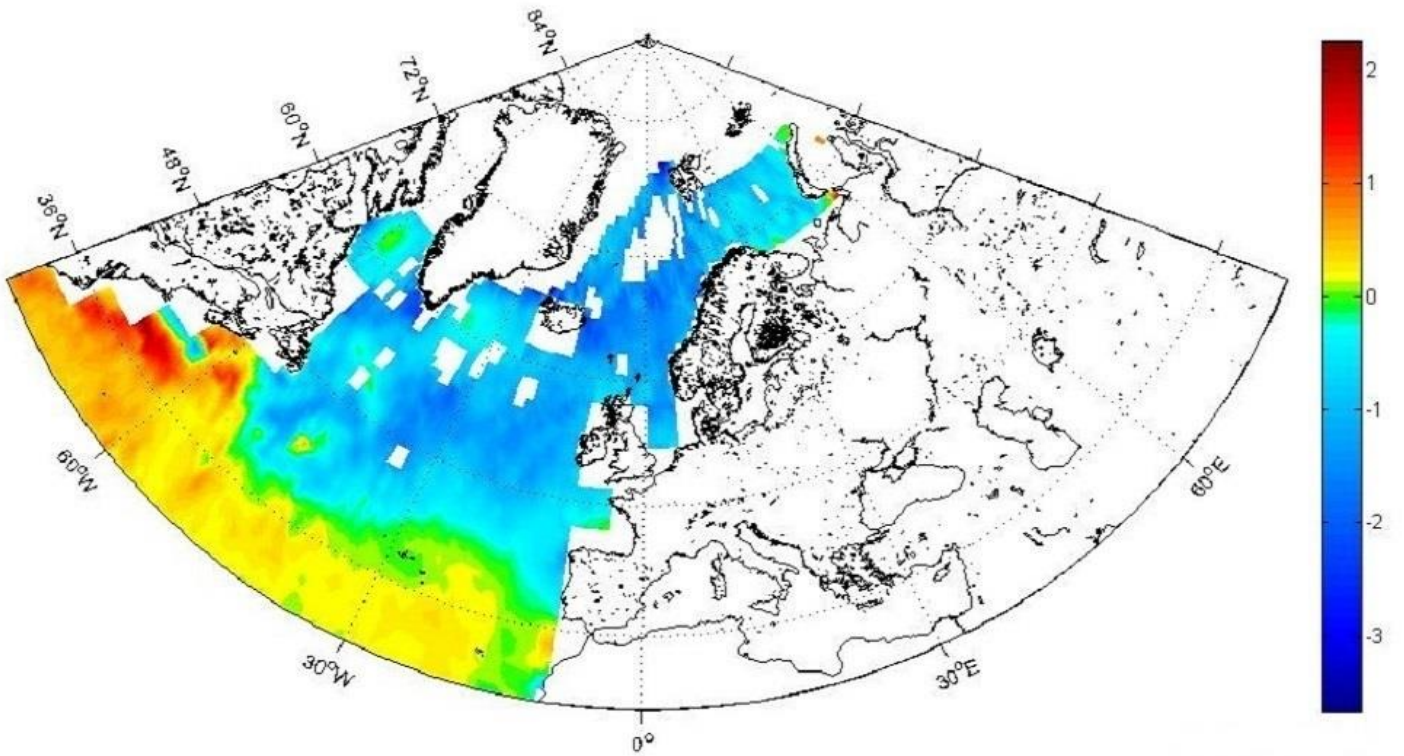
806 (mg C m⁻² day⁻¹)
807
808

809
810 c)



(mg C m⁻² day⁻¹)

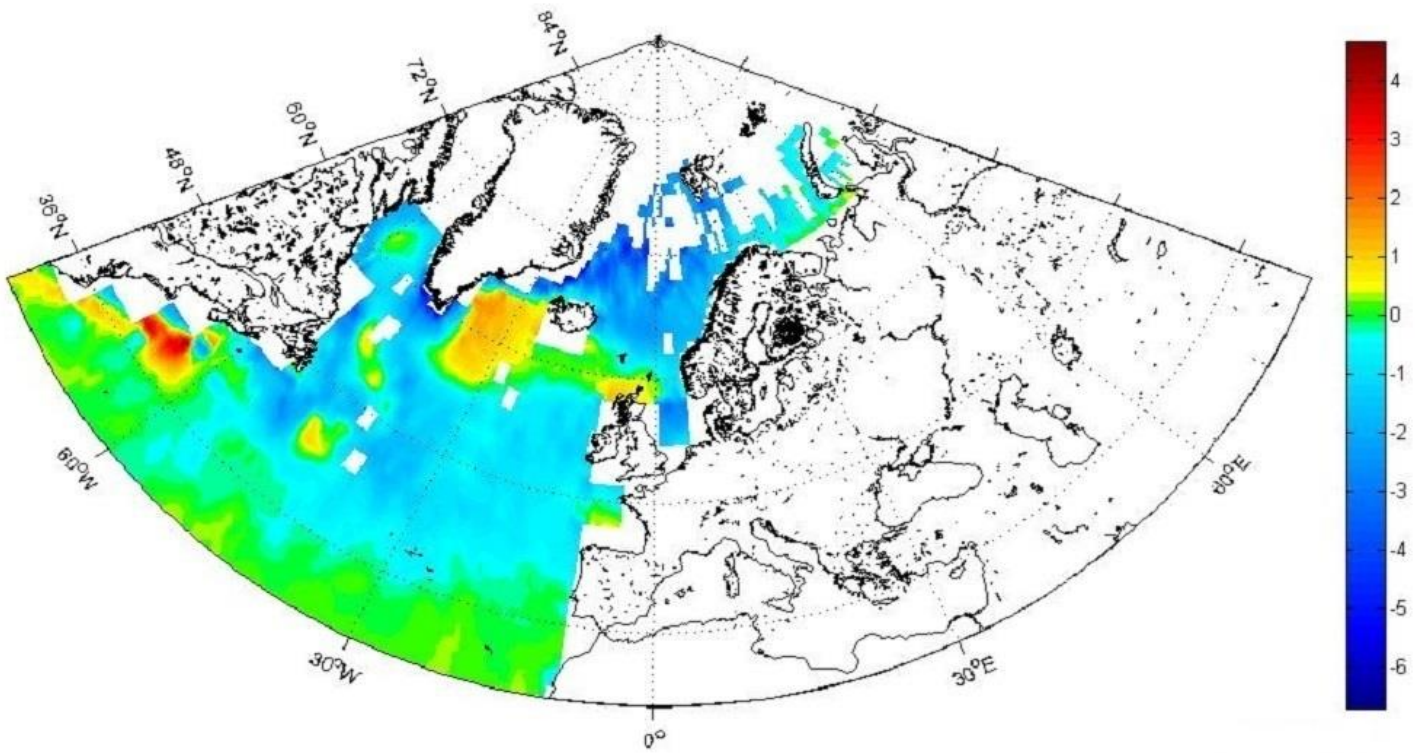
811
812 d)



(mg C m⁻² day⁻¹)

813
814
815

816
817 e)

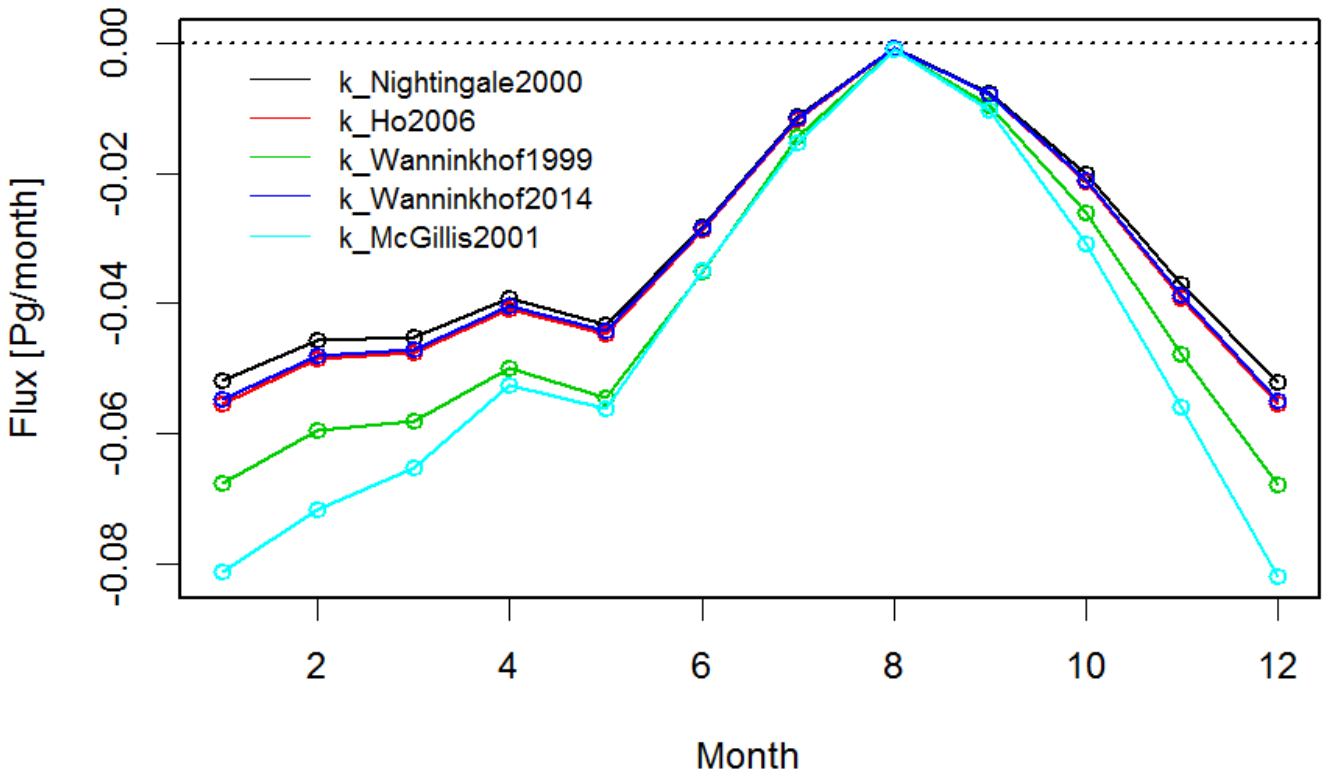


818 (mg C m⁻² day⁻¹)

819
820 Figure 5. Differences maps for the air-sea CO₂ fluxes (mg C m⁻² day⁻¹) in the North Atlantic, between
821 a cubed and a squared parameterization (Wanninkhof and McGillis 1999 and Wanninkhof 2014) a)
822 annual, b) DJF (winter), c) MAM (spring), d) JJA (summer), e) SON (autumn). The gaps (white
823 areas) are due to missing data, land and ice masks.

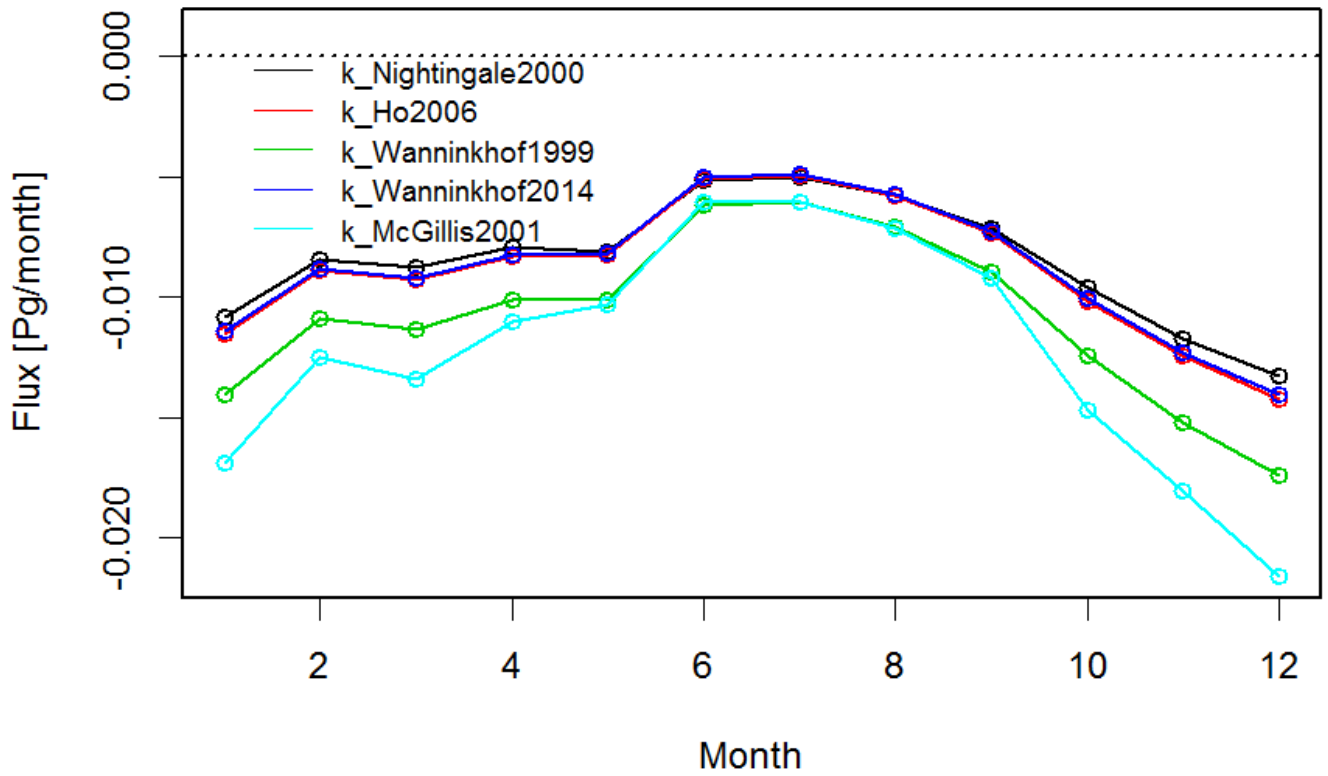
824
825

a)



826
827

b)

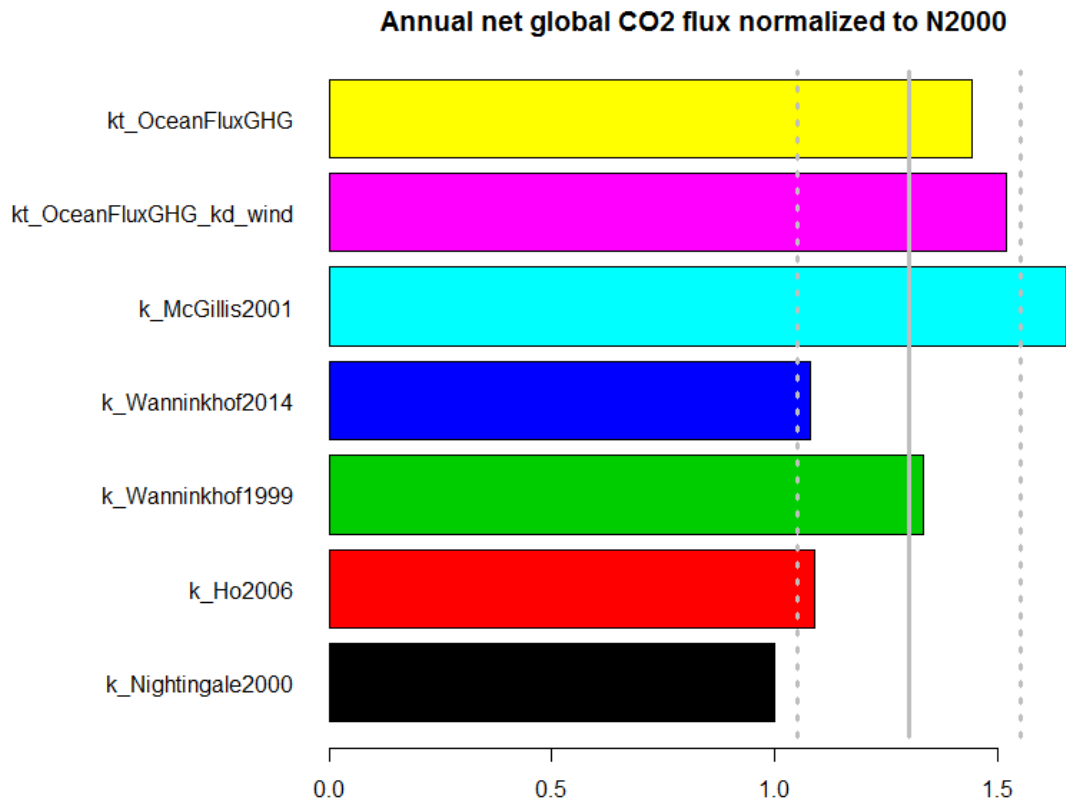


828
829
830
831

Figure 6. Monthly values of CO₂ air-sea fluxes (Pg/month) for the five parameterizations (eq. 4-8) a) the North Atlantic, b) the European Arctic.

832

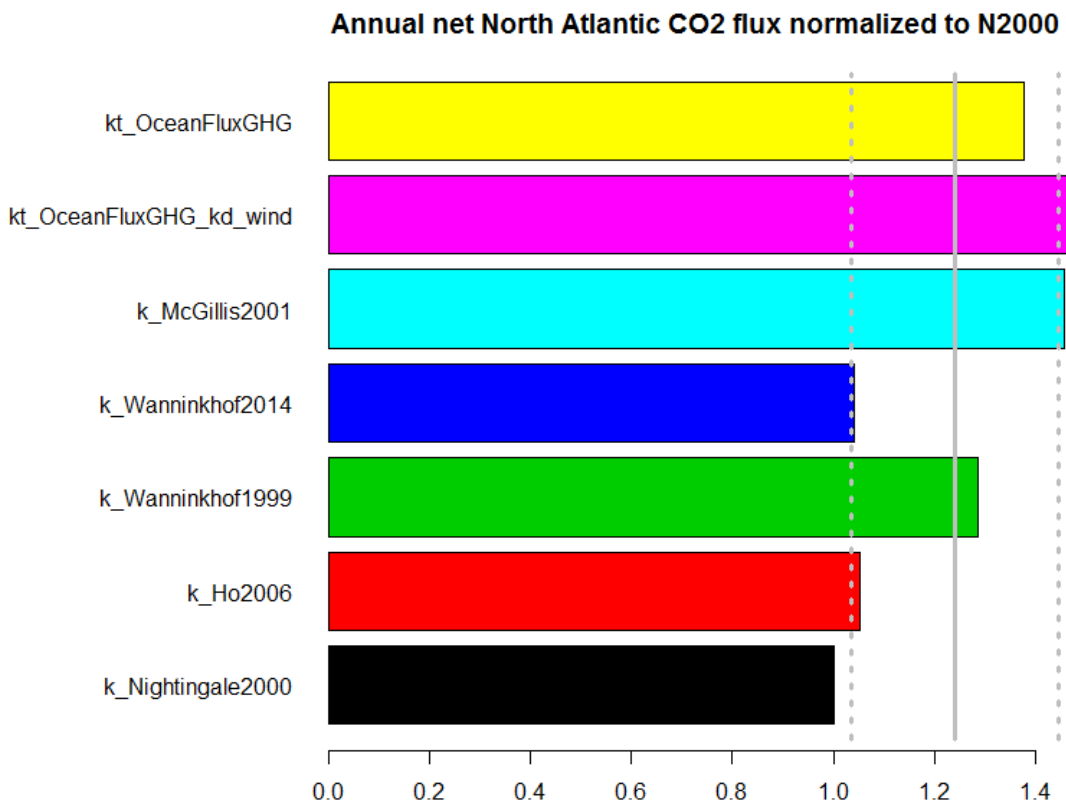
833 a)



834

835

836 b)



837

838

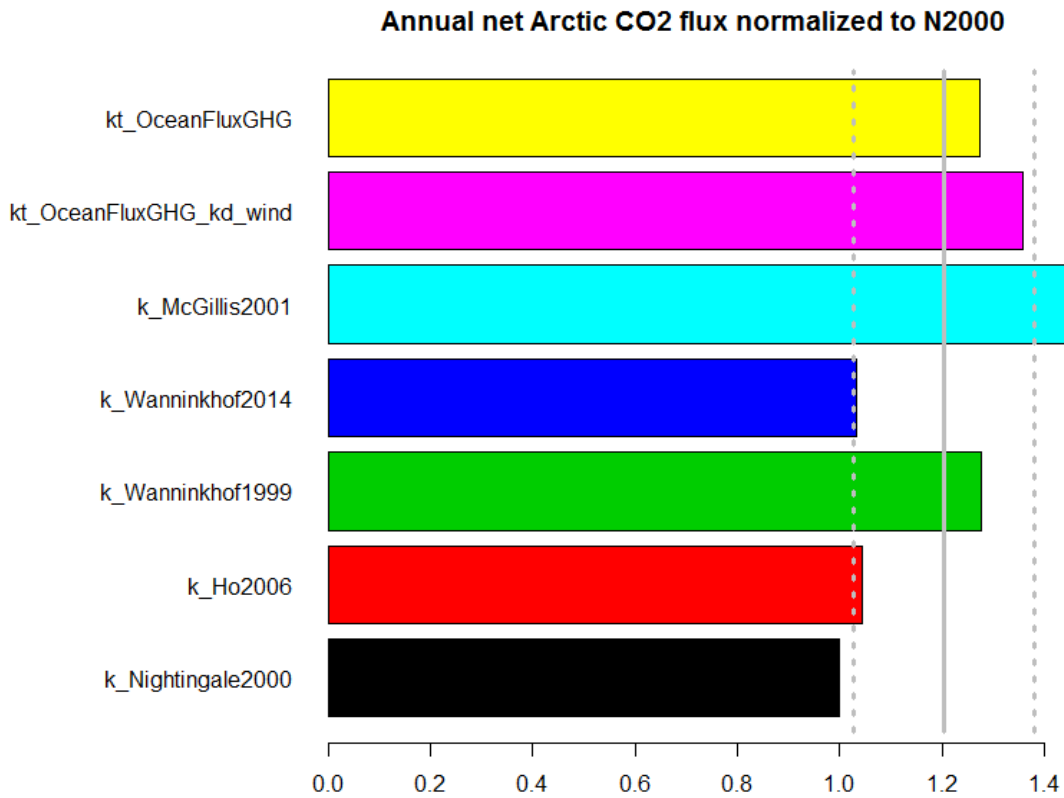
839

840

841

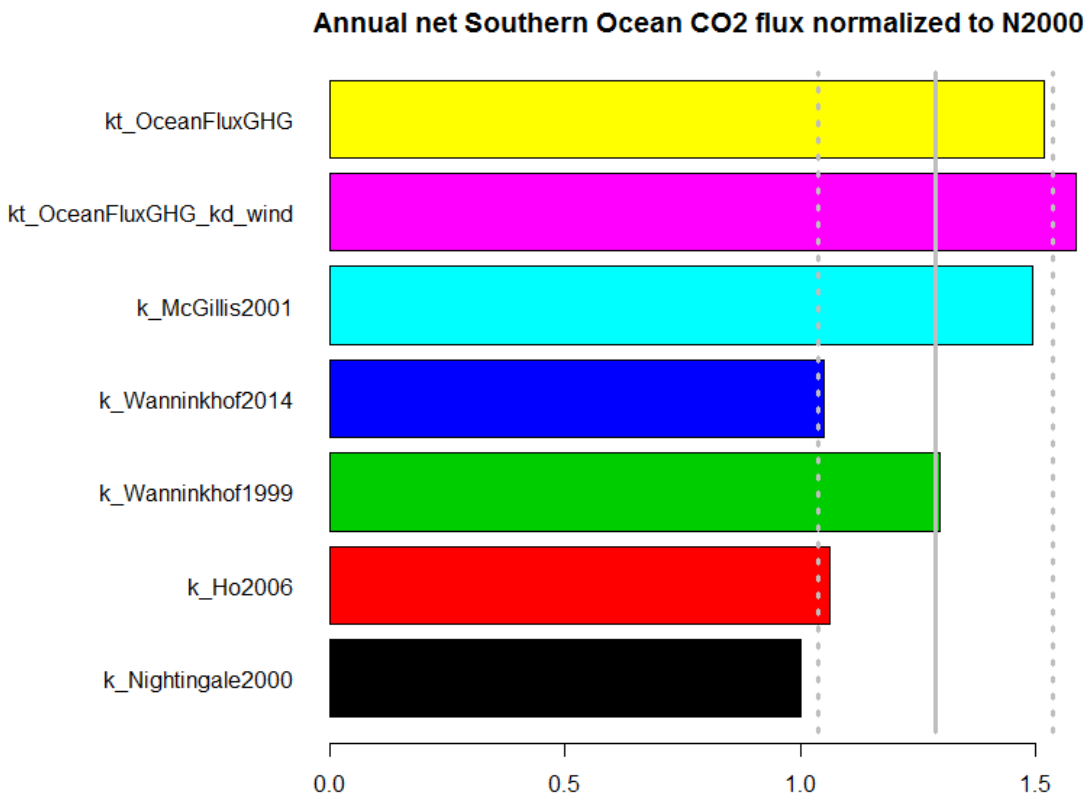
842

843 c)



844

845 d)



846

847

848

849

850

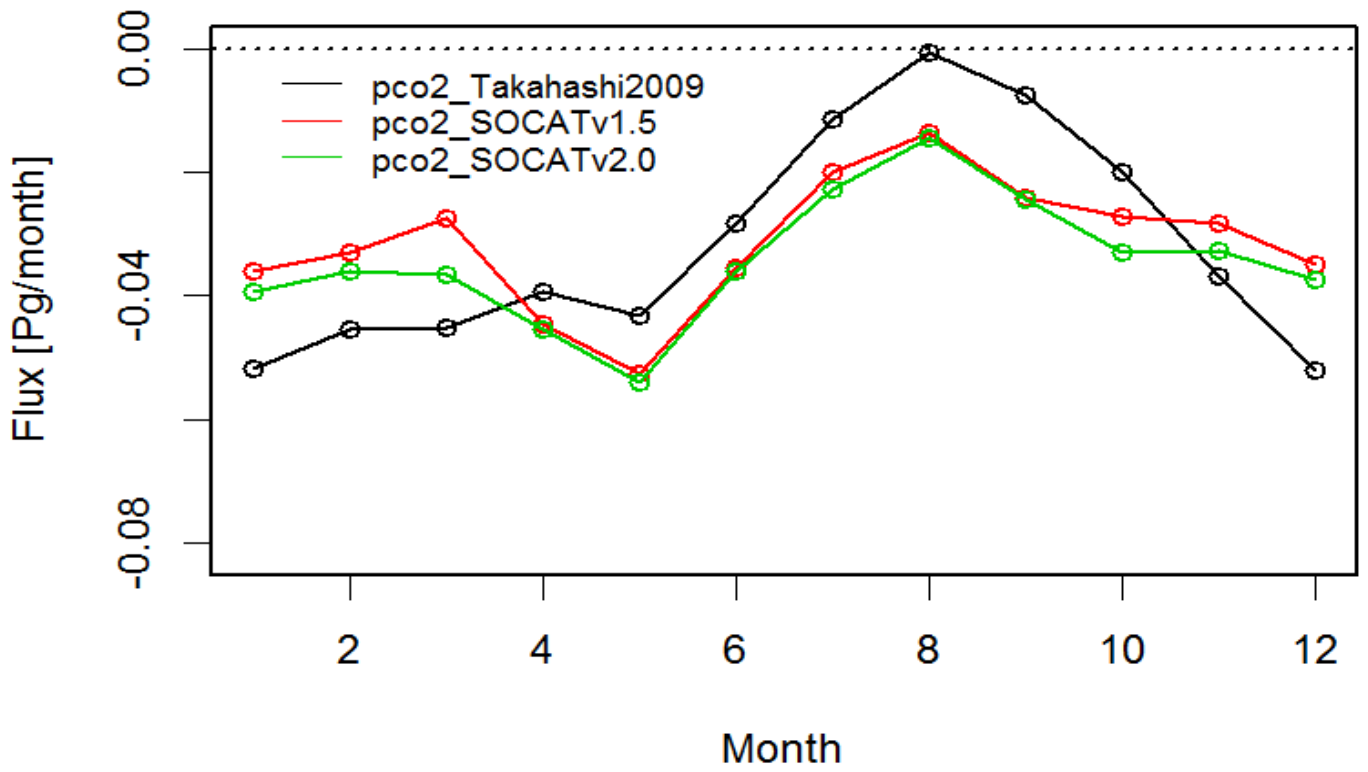
851

Figure 7. Annual air-sea fluxes of CO₂ for the five (eq. 4-8) parameterizations as well as for backscatter (default) and wind driven OceanFluxGHG parameterizations normalized to flux values of Nightingale et al. (2000) *k* parameterization (see text) a) globally, b) the North Atlantic, c) the European Arctic, d) the Southern Ocean. Average values for all parameterization and standard deviations are marked as vertical gray lines.

852

853

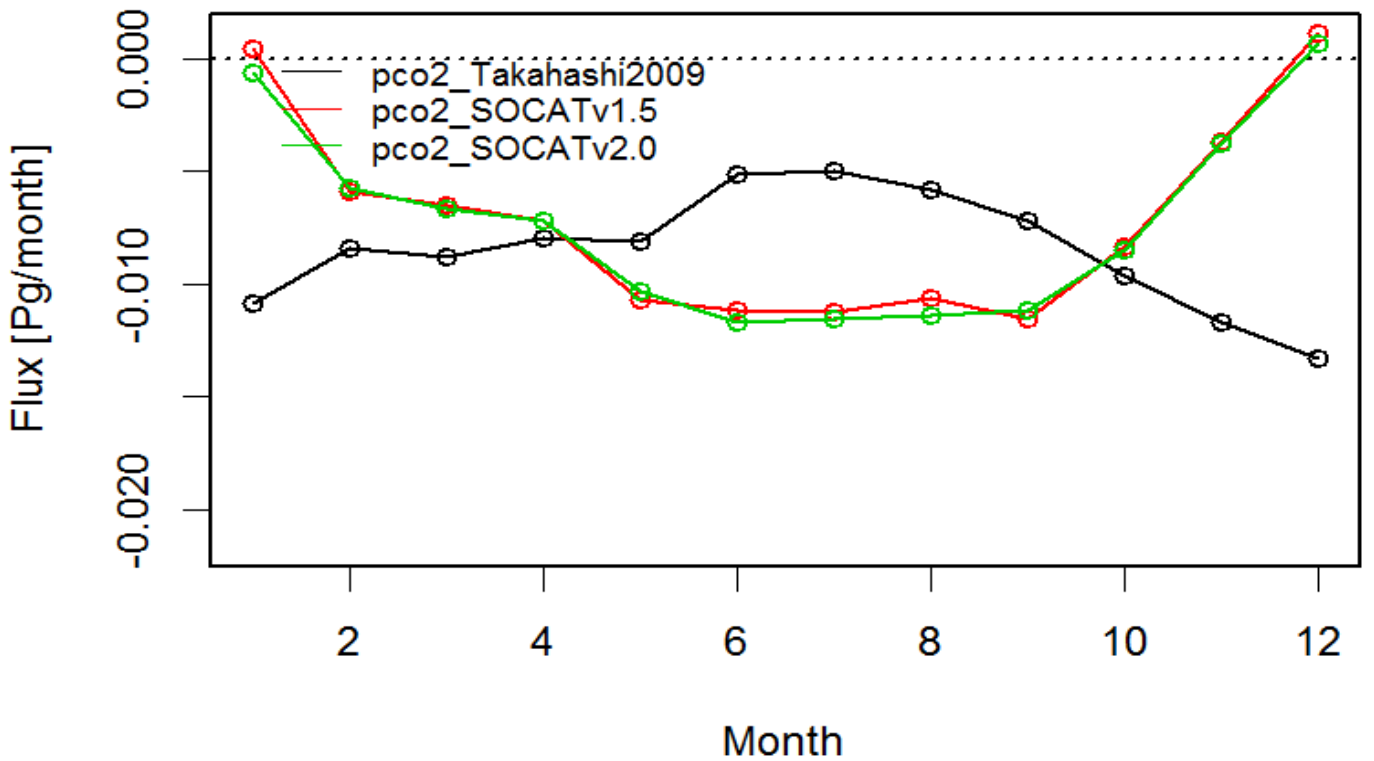
a)



854

855

b)



856

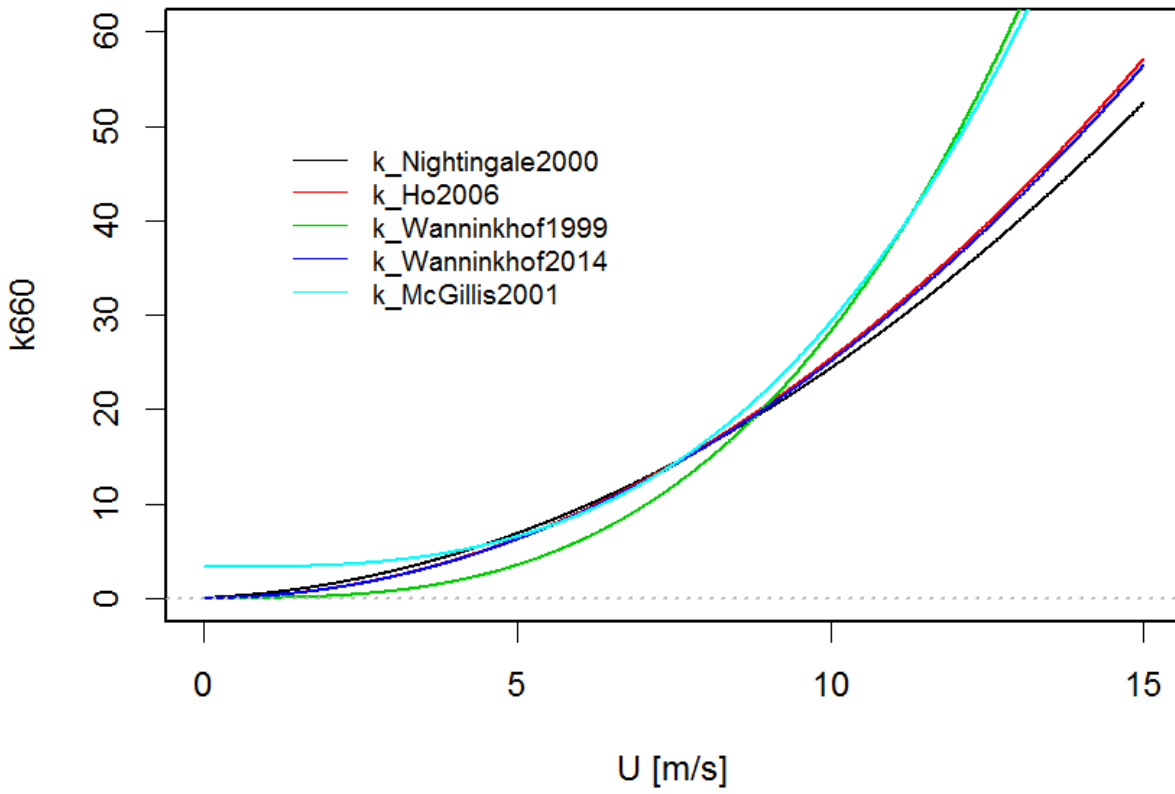
857

858

859

Figure 8. Comparison of monthly air-sea CO₂ fluxes calculated with different *p*CO₂ datasets (Takahashi et al., 2009, SOCAT v. 1.5 and 2.0) using the same *k* parameterization (Nightingale et al., 2000) a) the North Atlantic, b) the European Arctic.

860
861



862
863 Figure 9. Different k660 parameterizations as a function of wind speed.